universität wien

DIPLOMARBEIT

Titel der Diplomarbeit

Hoch zytotoxische Kupfer(II)-Komplexe modifizierter Paullon-Liganden

Verfasser

Michael F. Primik

angestrebter akademischer Grad

Magister der Naturwissenschaften (Mag. rer. nat.)

Wien, November 2009

Studienkennzahl lt. Studienblatt:	A 419
Studienrichtung lt. Studienblatt:	Diplomstudium Chemie
Betreuerin / Betreuer:	Ao. Univ. Prof. Dr. Vladimir B. Arion

universität wien

DIPLOMA THESIS

Title of the thesis

Highly Cytotoxic Copper(II) Complexes with Modified Paullone Ligands

Author

Michael F. Primik

Supervisor

Ao. Univ. Prof. Dr. Vladimir B. Arion

Vienna, November 2009

To my family

Acknowledgements

Here I want to thank all people who contributed to the success of this work:

O. Univ.-Prof. Dr. Dr. Bernhard K. Keppler for the opportunity to work in his group on this highly interesting topic and his generous support.

My supervisor Ao. Univ.-Prof. Dr. Vladimir B. Arion for his gorgeous support and patience, as well as for all the proofreading, many fruitful tips and discussions and the refinement of X-ray structures.

Ao. Univ.-Prof. Dr. Markus Galanski for the collection of 2D-NMR data.

Dr. Michael Jakupec and Gerhard Mühlgassner, MSc. for running the biological tests and accordant evaluation.

The NMR service team (Mag. Sergey Abramkin, Dr. Wolfgang Kandioller, DI Amitava Kundu) for measuring the numerous spectra.

Mag. Anatolie Dobrov for ESI mass spectrometry measurements and Ing. Alexander Roller for collecting the X-ray data.

Mag. Werner Ginzinger for many fruitful conversations and help with computational problems.

Dr. Wolfgang Kandioller, Dr. Christian Kowol and Mag. Anatolie Dobrov for their tips and conversations.

My laboratory partners Dr. Christian Kowol, Mag. Anatolie Dobrov, Mag. Aliona Luganschi for the pleasant atmosphere and talks.

Mag. Elfriede Limberger and Mihai Odoleanu for enabling frictionless work by untiringly tackling all kinds of administrative problems.

My friends, working group partners and study colleagues Verena Pichler, Andrea Kurzwernhart and Lukas Filak for having five great years.

The whole working group for pastries and cookies, coffee, crossword puzzles, barbecues, happy hours, etc.

Prof. Dr. Franz Scherr for showing me the way to chemistry and the Austrian Chemistry Olympiade.

My parents and my sister for their unquestionable support throughout my whole life.

Manuela for the last five years, and many more to follow.

Abstract

Cancer diseases are the second most common cause of death in Austria and third worldwide. Therefore much attention has been given to cancer research and therapies over the last decades. Beside surgery and radiation therapy, chemotherapy is the most common treatment of cancer. In almost 50% of incidences the platinum based drugs cisplatin, carboplatin and oxaliplatin are used to cure the diseases. Related side effects, such as nephrotoxicity, neurotoxicity, nausea, vomiting, etc. are the main disadvantages. A growing chemoresistance to these classical drugs is another stimulus to overcome these problems. Consequently the focus of researchers turned to other metal ions as coordination centres. Especially complexes of gallium(III) (e.g. KP46) and ruthenium(III) (e.g. NAMI-A, KP1019), which imitate the properties of iron in biological systems, show promising antiproliferative activities even though they are less cytotoxic than the platinum based drugs.

Another promising approach to new chemotherapeutics is the coordination of biologically active ligands to metal ions. Indolo[3,2-*d*][1]benzazepines (paullones) were found to be potent inhibitors of Cyclin dependent kinases (CDKs), enzymes controlling the cell cycle progression. Especially Kenpaullone exhibits an activity profile similar to Flavopiridol, which is a well known inhibitor of the CDK1-cyclinB complex. Nonetheless the poor bioavailability of the paullones remains a limiting factor for application. Coordination of paullone derivatives to ruthenium and osmium resulted in higher solubility in aqueous media and increased cytotoxicity. However, ruthenium and osmium are not essential trace elements. Therefore we focused our attention on complexes of the biocompatible first row transition metals.

The aim of this work was the synthesis and characterisation of copper complexes of paullone-based ligands, their characterisation by available techniques and cytotoxicity tests with respect to the antiproliferative activity of the newly synthesised compounds.

Zusammenfassung

Krebserkrankungen stellen heute die zweithäufigste Todesursache in Österreich und bereits die dritthäufigste weltweit dar. Dem entsprechend hat sich auch die Krebsforschung weiterentwickelt. Zu den heute angewandten Standardtherapien zählt neben Chirurgie und Strahlentherapie vor allem die Chemotherapie. Beinahe die Hälfte der Krankheitsfälle wird mit den platinhältigen Medikamenten Cisplatin, Carboplatin und Oxaliplatin behandelt. Die auftretenden Nebeneffekte wie Nephro- und Neurotoxizität, Übelkeit und Erbrechen zählen zu ihren großen Nachteilen. Zusätzlich können im Verlauf der Behandlung Resistenzen gegen die Therapeutika auftreten. Darum konzentriert sich die Forschung zunehmend auf die Entwicklung von Medikamenten, die auf anderen Metallionen basieren, um den auftretenden Nachteilen platinhältiger Medikamente entgegenzuwirken. Speziell die Komplexe der dreiwertigen Ionen des Galliums (z.B. KP46) und Rutheniums (z.B. NAMI-A, KP1019), die Eisen in biologischen Systemen nachahmen, zeigen vielversprechende antiproliferative Aktivität, obwohl sie weniger zytotoxisch sind als die bereits angewandten Platinverbindungen.

Die Koordination biologisch aktiver Liganden an Metallionen ist ein ebenfalls vielversprechender Ansatz. Indolo[3,2-*d*][1]benzazepine (Paullone) hemmen Zyklin abhängige Kinasen (CDKs), Enzyme die den Zellzyklus kontrollieren. Speziell Kenpaullon ähnelt in seiner Aktivität Flavopiridol, einem bereits bekannten Inhibitor des CDK1-cyclinB Komplexes. Die geringe Bioverfügbarkeit der Paullone bleibt ein beschränkender Faktor. Die Koordination von Paullonderivaten als Liganden an Ruthenium und Osmium hat bereits zur Lösung des Problems beigetragen (höhere Löslichkeit in wässrigen Medien, höhere Zytotoxizität), aber da es sich bei Ruthenium und Osmium nicht um Spurenelemente handelt, wurde der Fokus auf Ionen von biokompatiblen Elementen der ersten Übergangsmetallreihe gerichtet.

Ziel dieser Arbeit war die Synthese und Charakterisierung von Kupfer-Komplexen mit Paullonderivaten als Liganden, sowie Zytotoxizitätstests.

Table of Contents

Abbreviations

DNA	deoxyribonucleic acid
CDK(s)	cyclin dependent kinase(s)
CAK(s)	CDK-activating kinase(s)
$p19^{INK4d}$	protein from the INK4 family of CDK inhibitors (also known as CDKN2D)
TF(s)	transcription factor(s)
Ser	serine
Thr	threonine
ATP	adenosine triphosphate
pRb	retinoblastoma protein
ATC	Anatomical Therapeutic Chemical Classification System
tf	transferrin
ROS	reactive oxygen species
RNR	ribonucleotide reductase
dNTP(s)	deoxyribonucleotide(s)
IC_{50}	half maximal inhibitory concentration
HSA	human serum albumin
RNA	ribonucleic acid
PKC	protein kinase C
NMR	nuclear magnetic resonance
HSAB	hard and soft acids and bases
AA	amino acid

1. Introduction

Today cancer is one of the main causes of death in the world. Being the third in line after cardiovascular and infectious & parasitic diseases, malignant neoplasms caused 7.3 million deaths worldwide in 2007 – this is 13% of worldwide deceases.[1] The World Health Organization (WHO) predicts that mortality from cancer will rise continuously and will achieve 12 million casualties worldwide in 2030.[1]

The situation is different in the industrial countries, of which Austria is chosen as an example. Deceases from infectious & parasitic diseases have decreased continuously for decades and cause just 1% of all deaths nowadays. Cancerous diseases are the second most lethal diseases in Austria only outnumbered by cardiovascular ones. About one out of four deaths is caused by the malignant neoplasms. Consequently the mortality rate is twice as high as it is worldwide.

Cause of death, %	**Worldwide 2004**		**Austria 2008**	
	Female	Male	Female	Male
Cardiovascular diseases	31.5	26.8	48.0	37.3
Infectious and parasitic diseases	15.6	16.7	0.8	0.9
Cancer	11.8	13.4	23.1	30.0

Table 1: Comparison of leading causes of death worldwide[1] and in Austria.[2]

It is noteworthy that the incidence of different types of cancer differs between the two genders. The leading malignomas in women are those of breast, colon, uterus and lung, whereas men frequently come down with cancers of prostate, colon, lung and bladder. It should also be mentioned in this context that between 1983 and 2006 the incidence of malignant neoplasms in Austria increased from 29500 to 37000 (+25%)[3], whereas the related deaths remained constant at about 19000 per year.[3]

Keeping in mind all these facts it becomes clear that the fight against cancer will be a major task for medicinal and biochemical research for decades to come.

2. Carcinogenesis and Cell Cycle Control

2.1 Carcinogenesis

Carcinogenesis (emergence of cancer) is often a long-term process of the transformation of healthy cells into cancer cells. Its initiation starts with a single mutation in a gene of a differentiating cell. This DNA mutation can be induced by endogenic or exogenic factors. Endogenic factors are determined by genetic predisposition e.g. a protooncogene or a tumour supressor gene. Its mutation leads to cancerous growth. Protooncogenes act in a dominant manner. If a mutation takes place in a protooncogene it turns into an oncogene whose protein products support uncontrolled cell proliferation. Tumour suppressor genes inhibit malignant proliferation as long as they are not mutated too. Mutated tumour suppressor genes lose their functionality. However, as they act in a recessive way both alleles (genomic copies of the gene) must be changed first. Exogenic factors can be biological (e.g. HPV, HIV), physical (e.g. UV and radioactive radiation) or chemical (nutrition, smoking, asbestos, vinyl chloride, polycyclic aromatic hydrocarbons, etc.). They are responsible for nearly 80% of all incidences.

If repair mechanisms fail and the mutation is set, initiation is irreversible and tumour promotion progresses. This period can last for years. Within the affected cells additional mutations accumulate during subsequent years. Thereby the cells develop altered properties to make themselves capable of cancerous growth:[4] Self-sufficiency in growth signals, insensibility to anti-growth signals, tissue invasion & metastasis, limitless replicative potential, sustained angiogenesis and evading apoptosis are the main properties of a cell capable of cancerous growth (Fig. 1a). Nonetheless, it must be noted that even though the mutations are irreversible, they still can be deleterious and lead to the death of the cells. Accordingly, it is required for the affected cells to maintain a determined level of genetic instability. In healthy cells, the level of genetic instability is low (Fig. 1b, A). As a consequence these cells are not likely to be mutable enough to end up as further proliferating cells when they are to hit a selection barrier (for instance low oxygen levels or a deficiency of proliferation signals). In tumour precursor cells the level of genetic instability is higher (Fig. 1b, B). Thus it is probable that at least one cell will be genetically capable to overcome the barrier and promote the tumour progression further. The responsible genetic instability can be

tracked down in the lineage of the tumour. Genetic instability is too high (Fig. 1b, C), if deleterious mutations occur, resulting in either a slower proliferation rate or elimination of the affected cells. Consequently the tumour cell lineage can become extinct.

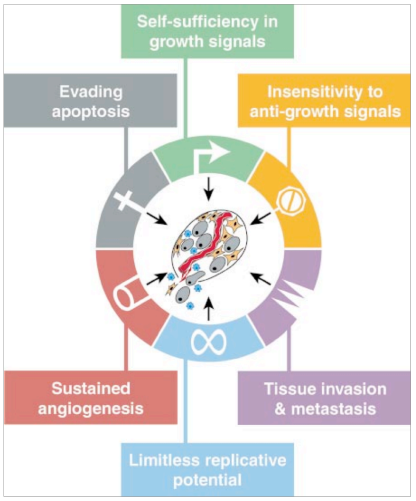

Figure 1a: Six key properties of a cell capable of cancerous growth.[4]

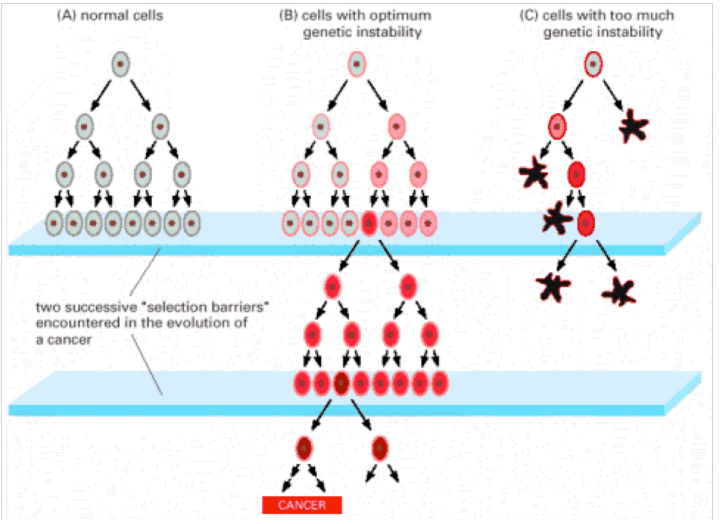

Figure 1b: Genetic instability and tumour progression.[6]

The final step is tumour progression when a former benign tumour becomes a malignant one and starts to invade the surrounding tissue (Fig. 2). Subsequently the tumour has to ensure its maintenance with nutrients and thus forms blood vessels (angiogenesis) by itself. In later stages cells leave the primary tumour and form secondary tumours (metastasis) in other tissues. In 50% of human tumours proliferation is accompanied by the mutation of the tumour suppressor gene p53. It is a gene coding for the same-named TF involved in cell cycle control and apoptosis (programmed cell death).

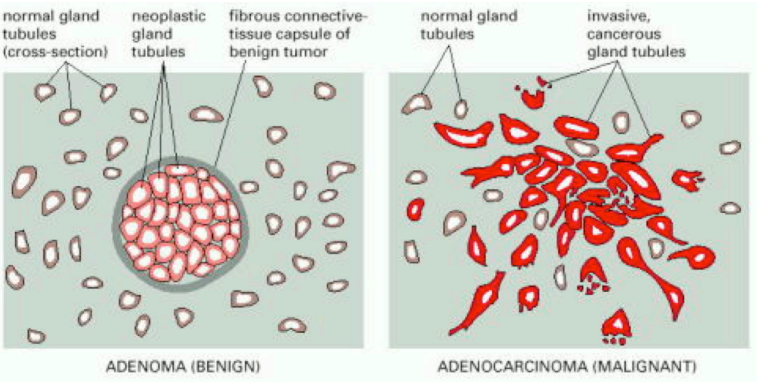

Figure 2: Benign versus malignant tumours.[6]

2.2 The Cell Cycle[5, 6]

The time a cell needs to replicate and divide into two daughter cells is called the cell cycle. It is divided in different phases: the quiescent phase (G_0), interphase (G_1, S, G_2) and the mitotic phase (M) (Fig. 3a). In G_1-phase (gap) the cell grows and proteins necessary for DNA replication are expressed. In S-phase (synthesis) DNA is replicated, and RNA and proteins are synthesised as well. G_2 phase serves as preparation for mitosis (nonetheless protein and RNA synthesis is carried out in G_2 phase too). Mitosis and cytokinesis are performed in M phase. Not all cells pass the cell cycle at the same speed or the same time, respectively. Liver cells for instance undergo mitosis just once a year, nerve cells never, but epithelial cells or the precursor cells of blood cells almost once a day. Additionally, cells posses the opportunity to exit the cell cycle and arrest in the quiescent or senescent G_0 phase. This is done when a cell is fully differentiated or growth factors and nutrition are present insufficiently. As long as the cell is not fully (terminally) differentiated, addition of growth factors and nutrition allows the cell to reenter the cell cycle.

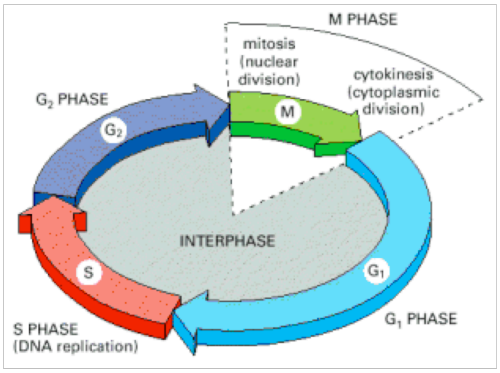

Figure 3a: The phases of the cell cycle.[6]

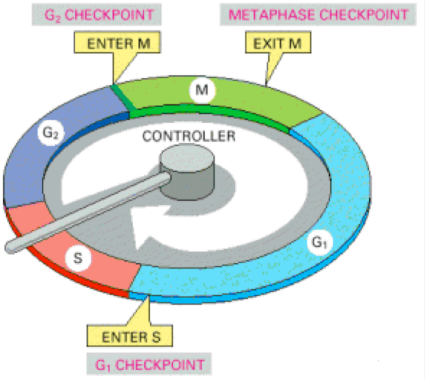

Figure 3b: The three cell cycle checkpoints.[6]

The cell cycle is based on strict control mechanisms set between the different phases, as it is inevitable to finish a cell cycle phase before starting the next one (Fig. 3b). It would be disastrous for a cell to enter S phase before finishing the synthesis of nucleotide building blocks in G_1 phase, which are necessary for DNA replication. There are three checkpoints. The first in late G_1 phase controls the cell's size and the accuracy of the genome. If no repairs have to be carried out the cell may progress into S phase. The second in G_2 phase reviews the newly replicated pieces of DNA on damages and suspends the cell cycle if necessary. The third in M phase controls the

distribution of the chromosome sets within the mitotic spindle. The decision whether a cell may pass a checkpoint or not is determined by external growth factors as well as by a group of intracellular protein kinases: the cyclin dependent kinases (CDKs).

2.3 Protein Kinases

There are about 850 kinases encoded within the 30000 genes of the human DNA.[7] Kinases are enzymes (biological catalysts) phosphorylating their target molecules. For instance binding of a kinase to a G-protein coupled receptor often induces a signal cascade within the cell, based on conformational changes of the involved proteins caused by targeted phosphorylation.

Thus protein kinases constitute major pharmacological targets, as very often signal transduction pathways are altered in several diseases. Especially phosphorylation of serine, threonine and tyrosine residues exhibits a key role in inevitable functions of cell life. Among the Ser/Thr kinases, the CDKs are of special interest because they are the pacemakers of cell-cycle control.[7] These kinases are dependent of assembling with cyclin proteins to form an enzymatic active complex. There are thirteen different CDKs and 25 proteins with homology in the cyclin box encoded in the human genome.[7] An example: in the middle of G_1-phase the CDKs 4 and 6 associated with cyclin D are activated by extracellular signals. These complexes phosphorylate (by consumption of ATP as phosphate donor) the retinoblastoma protein (pRb). As a consequence pRb is inactivated. This leads to the release of the TFs E2F and DP1, which monitor the expression of genes necessary for the G_1/S transition and S phase progression.[7]

Now how is p53 connected to the CDKs? In normal cells p53 protein is associated with Mdm2 protein and its cellular level is low (Fig. 4). If DNA damages are detected, p53 gets phosphorylated and its cellular level rises. This activated p53 enhances the transcription (as a TF) of protein p21, which associates with the CDK4-cyclin D complex leading to its inhibition. Thus no E2F and DP1 are released and the cell arrests in G_1. In 50% of all cancer cells the p53 gene is mutated. Consequently the p53 protein loses its functionality and DNA damages cannot be repaired anymore (following this important repair mechanism). Furthermore the cell will not exit the cell cycle and

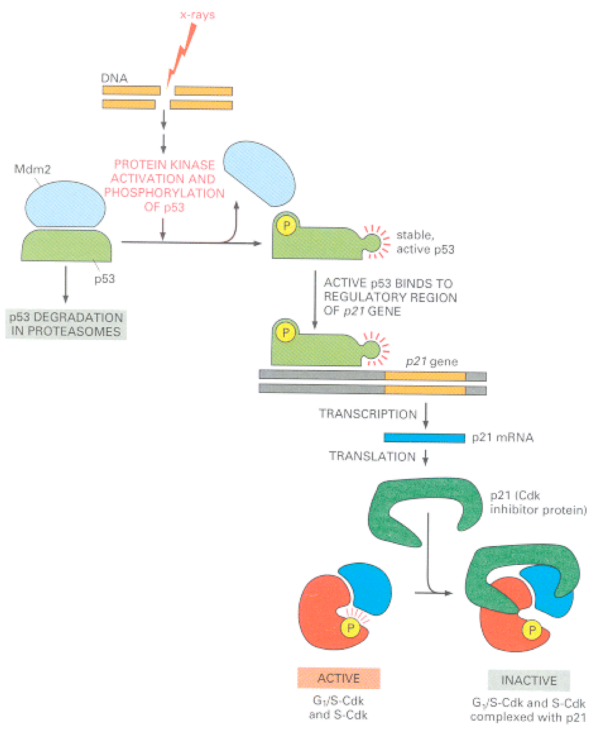

arrest, but progress and through mitosis the mutated genes will be inherited to the subsequent daughter cells.[8]

As CDK deregulations appear frequently in cancers,[9] much attention has been focused on the development of pharmacological inhibitors of CDKs.[10]

Figure 4: The G_1 checkpoint mechanism including p53.

3. Cancer Therapy

Standardised medicinal treatment of cancers comprise of three therapeutic methods:

- Surgery
- Radiotherapy
- Chemotherapy

Surgery is the oldest technique. Its usage can be retraced down history, as it was already practiced in ancient Greece. Reasoned by more advanced means of detection (radiography, scintigraphy), surgery has become a front line method in the fight against cancer diseases. The unfortunate disadvantage is its limitation to solid, non-disseminating tumours.

In radiotherapy either X-ray or radioactive radiation is used. As in the case of surgery a non-disseminating, localised malignancy is necessary. It is also advantageous if the tumour is found close to the skin, but intraoperative radiation therapy is widely applied too. Nonetheless another disadvantage comes with radiation itself, as it can also be mutagenic.

Chemotherapy is the third standardised method for cancer treatment. In this context the term refers to antineoplastic drugs, but most generally it means the administration of chemicals in order to cure a disease. Classical chemotherapeutics cannot distinguish between healthy and malignant cells. The latter cells are in permanent need for nutrients as a result of their elevated metabolism. Consequently those cells will incorporate more nutrients, as well as more of the administrated drug than non-affected cells. Thus tumour cells get damaged, due to their increased proliferation rate. Unfortunately within this principle lies the intrinsic disadvantage of this oldest form of chemotherapy. The most frequent appearing side effects emerge because there are rapidly dividing cells under normal circumstances as well. The unwantedly targeted cells are especially those of bone marrow, digestive tract and hair follicles. Thus myelosupression (decreased formation of blood cells), mucositis (inflammation of the lining of the digestive tract) and alopecia (hair loss) come to light. To overcome these problems research has been focusing lately on cellular targets especially associated with cancer to specify future chemotherapeutics. On the other hand chemotherapy is the method of choice against disseminating, non-solid tumours (e.g. leukaemia), which are untreatable with surgery and radiation therapy.

The WHO classifies antineoplasitc agents according to the ATC[11] code as followed:

- Alkylating agents
- Antimetabolites
- Plant alkaloids and other natural products
- Cytotoxic antibiotics and related substances
- Other antineoplastic agents

Alkylating agents (e.g. chlorambucil) alter the DNA's methylation pattern. Thus gene expression is deleteriously changed and the affected cells go into apoptosis. Antimetabolites simulate metabolic structures. Consequently they compete for metabolising against the metabolite they imitate. Antifolates for instance compete with folic acid, which is an important substrate for proliferation. Plant alkaloids and other natural products mainly hinder mitosis by degradation of the microtubule system. An example of cytotoxic antibiotics is dactinomycin, which is also used as an immunosuppressive agent after operations. Among the several groups of other antineoplastic agents, monoclonal antibodies, the widely used platinum compounds or protein kinase inhibitors can be found. As the main part of this work deals with synthesis and characteri-

sation of metal complexes of protein kinase inhibitor derivatives, further metal-based and protein-interfering agents will be discussed in more detail.

3.1 Platinum-Based Compounds

Cisplatin, *cis*-diamminedichloridoplatinum(II), was first synthesised by Michele Peyrone in mid 19th century and subsequently known as Peyrone's chloride.[12] The pharmaceutical potential of the complex was not known until it was discovered by chance in 1969 by Barnett Rosenberg.[13] In a series of experiments Rosenberg examined the influence of an electric field on mitosis of bacteria. Instead of dividing, the bacteria (*E.coli*) grew to the 300-fold length, compared to bacteria growing in the absence of an electric field. Further investigations brought to light that this was not due to the electrical field, but due to *cis*-diamminedichloridoplatinum(II) and *cis*-diammineteтrachloridoplatinum(IV), the platinum(IV) analogue of cisplatin (Fig. 5, 1).[14]

It took until 1978 when the FDA approved cisplatin for clinical use. Thus it became the first metal-based chemotherapeutic. Through its application, advanced and metastatic testicular germ-cell cancer became highly curable. Also ovarian cancer responds strongly and furthermore cancers of lung, cervix, endometrium, bladder and oesophagus are treated with cisplatin. Unfortunately advanced diseases are rarely healable as the tumours can develop resistances throughout the therapy.[15]

The mode of action of cisplatin is not fully understood yet. The biologically active species were proved to be the mono and diaqua species $[Pt(NH_3)_2(OH_2)Cl]$ and $[Pt(NH_3)_2(OH_2)_2]^{2+}$.[16] The cellular uptake of cisplatin appears to be based on diffusion downwards along a chloride gradient and not by transport through protein channels. Inside the cells, where chloride ion concentration is below 100 mM, hydrolysis sets in, resulting in the substitution of the chlorido ligand by a water molecule. The aqua species reacts with other binding partners and thus coordinates to N7 of nucleobase guanine and rarer adenine, hence forming 1,2-intrastrand adducts, deforming the double helical structure of the DNA. Consequently, as DNA repair mechanisms are negatively altered in cancer cells, the cells go into apoptosis.

Unfortunately severe side effects limit the application of cisplatin. The worst of these

effects are nephrotoxicity (dose-limiting), ototoxicity, neurotoxicity (several cancers) and nausea. To overcome these secondary effects and growing resistances the search for other drugs was begun. Thus several platinum-based complexes were brought into clinical trials, but only one of these second generation platinum-drugs became approved worldwide (carboplatin; 2, Fig. 5)) and one (nedaplatin; 4, Fig. 6) regionally in Japan. Carboplatin, cis-diammine-(1,1-cyclobutanedicarboxylato)platinum(II) differs from cisplatin in its coordination sphere.

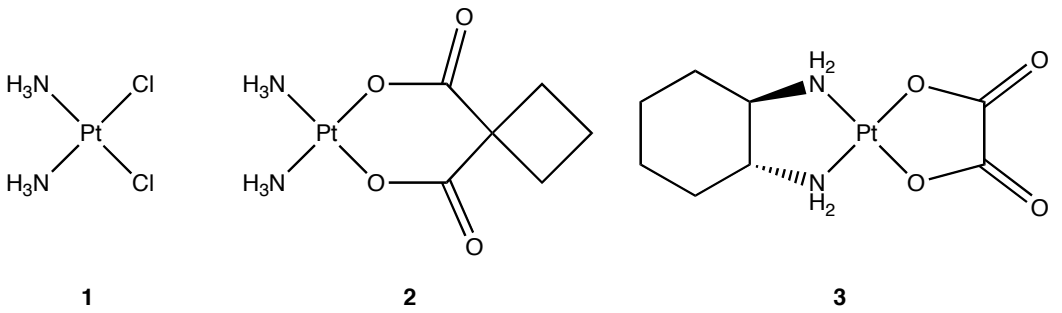

1 **2** **3**

Figure 5. Cisplatin (cis-diamminedichloridoplatinum(II)) (**1**), Carboplatin (cis-diammine-(1,1-cyclobutanedicarboxylato)platinum(II)) (**2**), Oxaliplatin ((1R, 2R)-diaminocyclohexane oxalatoplatinum(II)) (**3**).

The two chlorido ligands of cisplatin are exchanged for another leaving group, 1,1-cyclobutanedicarboxylate. Thus the appearing side effects are different as well. Myelosupression, especially thrombocytopenia, is the dose-limiting factor of carboplatin medication. In general carboplatin is less cytotoxic than cisplatin. Therefore 20-40 times higher doses must be administered. The DNA adducts formed are the same as in the case of cisplatin, but their formation rate is just one tenth in contrast to that of cisplatin.[17]

The third platinum-based antineoplastic drug approved for worldwide clinical use was oxaliplatin, (1R, 2R)-diaminocyclohexane oxalatoplatinum(II)[18] (Fig. 5, 3), from the group of third generation platinum(II)-drugs. The so-called DACH ligand (diaminocyclohexane), replaces the two ammine ligands of cisplatin and carboplatin. The resulting complex is well soluble in water.[15] The mode of action of oxaliplatin differs from that for the longer known platinum complexes, more precisely via the way it accumulates in cancer cells. The DNA adducts formed are the same[19] as for to cisplatin, but oxaliplatin appears to be a better inhibitor of DNA replication.[20]

About 40 platinum(II)-based compounds entered clinical trials, but just the three described before were approved for clinical use worldwide. Moreover just three other complexes were permitted nationally (Fig. 6): nedaplatin (4) in Japan, heptaplatin in South Korea (5) and lobaplatin in China (6). Further promising approaches focus on platinum(IV)-based drugs which will possibly be orally administered, due to the kinetic inertness of platinum(IV), whereas platinum(II)-drugs are limited to intravenous administration and thus connected with hospital stays for the affected people. One representative complex of this class of potential antineoplastic drugs is satraplatin (7, Fig. 6). Further trials of satraplatin application were abandoned after a clinical phase III study, which showed no substantial improvements in the overall survival rate.[21]

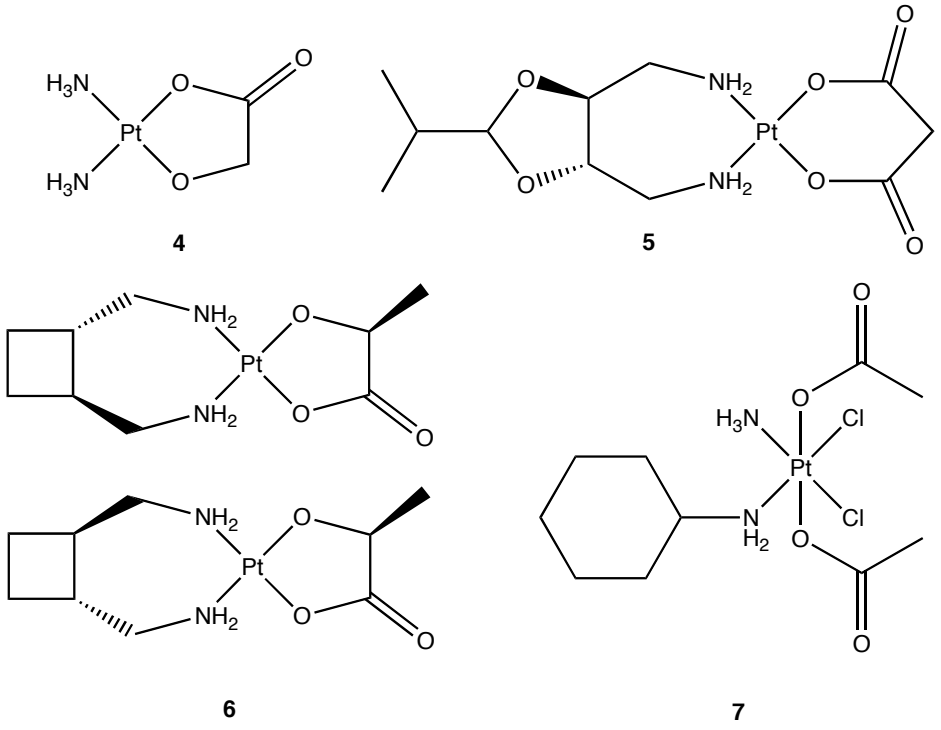

Figure 6. Nedaplatin, diammine-hydroxoacetato2--platinum(II) (**4**); Heptaplatin, [(4R,5R)-2(1-methylethyl)-1,3-dioxolane-4,5-dimethamine][propanedioato2-]platinum(II) (**5**); Lobaplatin, [(1R,2R)-1,2-cyclobutanedimethamine][2-hydroxypropanoato2]platinum(II) (**6**); Satraplatin, bis(acetate)-ammine-dichlorido-cyclohexanamineplatinum(IV) (**7**)

Efforts have also been focused on the investigation of resistances to cisplatin (and in lesser extent to carboplatin and oxaliplatin). The current knowledge concerning this subject was summarized in a review by Heffeter et al.[22] Based on the encountered restrictions accompanying the application of platinum-based drugs, researchers turned their attention to the development of novel metal-based agents.

3.2 Gallium-, Ruthenium- and Osmium-based Compounds

Currently applied platinum-based antineoplastic drugs face, additionally to the appearing side effects, commonly a growing resistance throughout their administration during chemotherapy in order to cure human cancer diseases at a disseminated state. The phenomena of “acquired” and “intrinsic” drug resistance of tumours is a serious problem. Acquired resistances are based on the tumour cells’ genetic instability, which allows a quick adjustment to chemotherapeutic lesions. Intrinsic resistances reflect properties of the tissue the tumour originated from. Especially epithelial cells are known to be protected against a life-long exposure to venoms.[22] As a natural consequence of these problems other prospective metal-based drugs have been designed, in order to reduce the platinum-linked side effects and to avoid the development of resistances.[23, 24]

3.2.1 Gallium

Gallium has been in frequent use for imaging in medicine. Its radioactive isotopes ^{67}Ga and ^{72}Ga concentrate in several tumour tissues, thus making gallium isotopes valuable tumour markers for radiation therapy as well.[25-27] In chemical respect Ga^{3+} imitates Fe^{3+} in many ways, for instance in electric charge, ionic radius and coordination number. Compared to the Fe^{2+}/Fe^{3+} redox-pair, Ga^{3+} exhibits no redox-activity under physiological conditions. Consequently it lacks a property significant for the role of iron in biological systems. Simulating the latter, Ga^{3+} is transported by transferrin (tf) protein as well and thereby enters cells embedded into this protein (tf binds to the tf receptor and is channelled into the cell susbsequently).

Cancerous cells are under permanent oxidative stress, due to their highly increased metabolism. Oxidative stress is caused by reactive oxygen species (ROS), which are side products of biologically occurring redox-processes. Hydrogen peroxide, superoxid and hydroxyl radicals belong to ROS. Natural systems have developed redox-proteins with embedded metal ions to handle metabolic redox-processes, as well as ROS. The functionality of these proteins is based on the redox-properties of the embedded metal ions, for instance Fe^{2+}/Fe^{3+} or Cu^{+}/Cu^{2+}. It is required that the redox potential of a redox-pair is accessible under physiological conditions (as it is for the two given before).

The increased metabolism of tumour cells requires more redox-proteins and thus higher amounts of the associated metal ions. To accumulate these metal ions, malignant cells express more receptors, i.e. tf receptor. The cellular uptake into the tumour of Fe^{3+} is accompanied by uptake of Ga^{3+}. Again the higher consumption of nutrients (in this case especially iron) by malignant cells (compared to normal ones) is responsible for the accelerated accumulation of Ga^{3+} in the tumour.

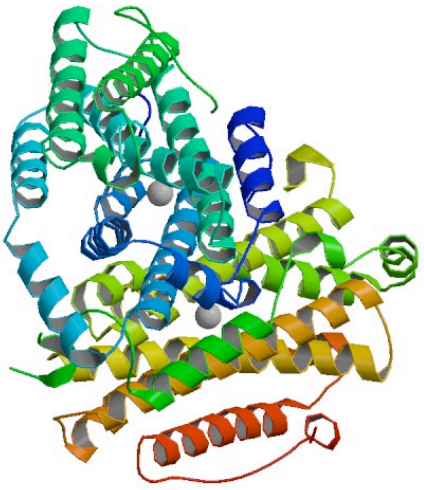

Figure 7. Human RNR, subunit M2 B[28]

It is commonly agreed that the major cellular target of Ga^{3+} is the enzyme ribonucleotide reductase (RNR, Fig. 7). This enzyme catalyses the reduction of ribonucleotides to deoxyribonucleotides (dNTPs), which are building blocks for DNA. Gallium substitutes the two Fe^{3+} ions in the active site of RNR, resulting in the enzyme's inhibition.

The first gallium-based compounds to enter clinical trials were gallium chloride, $GaCl_3$, and gallium nitrate, $Ga(NO_3)_3$.[29] As the last interacts with blood calcium levels, it was approved for the treatment of cancer associated hypercalcemia subsequently. Additionally occurring side effects such as nephrotoxicity[30, 31] (short treatment) and optic neuropathy and blindness[32] (continuous treatment) precluded further applications of gallium nitrate. Gallium chloride was withdrawn from clinical trials because of insufficient bioavailability.[33]

Gallium(III) complexes (Fig. 8) gallium maltolate (tris(3-hydroxy-2-methyl-4H-pyran-4-onato)gallium(III); 8) and KP46 (tris(8-quinolinolato)gallium(III); 9) appear to be more promising. Both compounds were synthesised for oral administration and are currently in clinical evaluation.[34] Thereby gallium maltolate has been tested versus refractory prostate cancer and multiple myeloma in a series of clinical phase I tests.[35] The same is true for KP46 which was tested against several refractory tumours.[36] The complexes differ from the salts in their behaviour in biological environment.

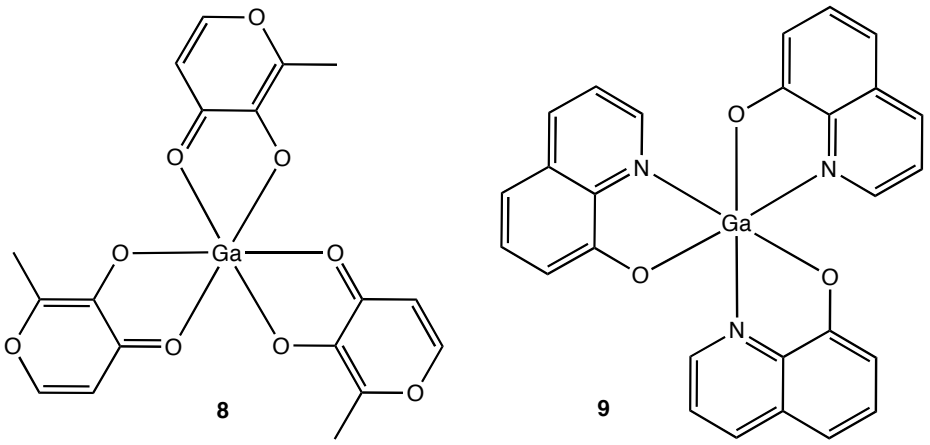

Figure 8. Gallium maltolate, tris(3-hydroxy-2-methyl-4H-pyran-4-onato)gallium(III) (**8**) and KP46, tris(8-quinolinolato)gallium(III) (**9**)

Gallium maltolate dissociates in the blood stream due to hydrolysis and the gallium ion is bound to transferrin subsequently. KP46 remains stable under the same circumstances and thus must follow a different way of absorption into the tumour.[34] Nonetheless bioavailability of the complexes remains manifold higher compared to the salts[37-39] and dose-limiting side effects do not appear.[35, 36]

Paullone-based ligands also were coordinated to Ga^{3+}, but insufficient solubility in biological media precluded their further development.[40, 41]

3.2.2 Ruthenium

Ruthenium is a second row transition metal placed below iron and above osmium. As osmium it belongs to the noble metals and consequently its chemical and physical properties differ from those of iron substantially. In contrast to iron the available oxidation states vary from +VIII to –II, with +II and +III as the most frequently appearing ones. Furthermore it is a chemically inert metal with respect to mineral acids. It is just soluble in aqua regia above 100°C. Of its seven natural isotopes ^{99}Ru and ^{101}Ru can be used for NMR measurements.[42]

Nonetheless ruthenium's vicinity to iron and its noble metal properties (related to platinum) make it an interesting candidate for metal-based drug development. Addi-

tional features concerning the metal's chemistry which play a role for the development of ruthenium-based antineoplastic agents are:[24]

- well known coordination chemistry and synthetic pathways,
- coordination geometry (octahedral),
- physiologically available oxidation states +II, +III, +IV,
- the ability to mimic iron in biological systems,
- a favourable ligand exchange rate. [24]

From the group of Ru(III) complexes, the most promising agents NAMI-A (imidazolium *trans*-[tetrachlorido(1H-imidazole)(DMSO)ruthenate(III)]; 10, Fig. 9) and KP1019 (indazolium *trans*-[tetrachloridobis(1H-indazole)ruthenate(III)]; 11, Fig. 9) have successfully passed clinical phase I trials and have begun (NAMI-A)[43], or are entering (KP1019)[44,45] phase II studies.

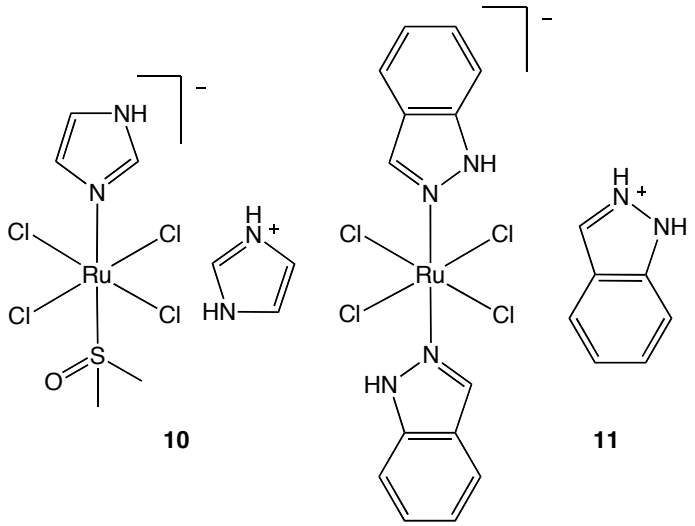

Figure 9. NAMI-A, imidazolium *trans*-[tetrachlorido(1H-imidazole)(DMSO)ruthenate(III)], (**10**) and KP1019, indazolium *trans*-[tetrachloridobis(1H-indazole)ruthenate(III)] (**11**)

These complexes are administered intravenously. Consequently they are dependent from transport proteins in the blood stream to reach their biological target. In contrast to gallium, these ruthenium(III)-drugs are preferentially bound to HSA[45] and only partially to transferrin.[46] Furthermore these complexes are thought to be pro-drugs, as their mode of action is described by the approach of "activation by reduction"[47] and thus they are categorised as functional compounds.[48] The permanent need for nutrients, due to high proliferation rate, accompanied by chaotic angiogenesis, put tumour

cells in a hypoxic state. As a result the primary energy source is anaerobic glycolysis yielding elevated amounts of lactate, which in its turn decreases the pH (acidifying) in the surrounding media.[48] In this more acidic environment the Ru(III) can be reduced by e.g. GSH or electron transfer proteins. Under these circumstances the t_{2g} orbitals of Ru(III) get filled, consequently elevating the electron density of the central metal ion and thus making the chlorido ligands replacement by water molecules easier. The intracellular targets of the compounds are thought to be DNA (N7 of guanine),[49] topoisomerases (inhibition) and mitochondria (direct interaction). Furthermore the complexes could be responsible for creation of ROS and are under investigation as metastasis inhibiting agents.[50]

Organo ruthenium(II) complexes have been developed recently. A special feature is the presence of a η^6-arene ligand[24,51] Compounds of this kind adopt a “three-leg” piano-stool geometry (Fig. 10).

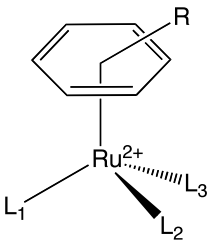

Figure 10. ‘Piano-stool structure’ of Ru(II)-arene complexes.

Generally the antiproliferative activity of these complexes can be tuned by the choice of appropriate ligands. In particular: several well known Ru(II)-piano-stool compounds were compared *in vitro* on A2780, an ovarian cancer cell line. The coordinated η^6-arenes differed from each other, but the other ligands remained the same. The complexes showed large differences in their antineoplastic activity profile. Coordination of e.g. tetrahydroanthracene decreases the IC_{50}-value of one complex twentyfold compared to coordinated p-cymene, which is the η^6-arene of choice as it exhibits a balance between cytotoxicity and solubility in biological media.[52] Of course cytotoxicity of the complexes can be tuned by derivatising the other three ligand positions. Thereby the generally pursued concept yields complexes with one mono- or bidentate ligand and two or one halides bound to the ruthenium(II), correspondingly. The halide part commonly forms the leaving group, whereas tuning of cytotoxicity is accomplished by means of the other ligand(s). Of the monodentate ligands the

RAPTA types are the most known. Bidentate ligands of the N,N-, N,O-, P,N-, S,O- or O,O- types were used. Paullone-based bidentate N,N-ligands with a bidentate N,N binding side have been coordinated to ruthenium(II) as well, but to them it will be referred later.[53-55]

3.2.3 Osmium

Generally its characteristics resemble those of ruthenium. As the latter, it is a noble metal and can be found in oxidation states from +VIII to –II as well. Unlike iron, the preferred oxidation state of osmium is +IV. Seven natural isotopes are known. Of those, ^{187}Os and ^{189}Os can be used for NMR measurements.[42]

Several properties distinct it from ruthenium, making it another interesting coordination centre.[42] Especially the altered ligand exchange kinetics, resulting from a stronger π-back donation of lower oxidation states and the much stronger spin-orbit coupling, are the most interesting features. It has been shown for complexes of the type $[M(maltolato)(H_2O)]^+$ (with M = Ru, Os) that the pK_a-values of the osmium complex is much lower, compared to its ruthenium analogue.[56] This is of importance, as the biological pH is about 7.40. As a result osmium complexes are more easily deprotonated in biological media than the ruthenium complexes. Deprotonation yields the less reactive [Os(maltolato)(OH)].[56] An osmium(II) η^6-arene (p-cymene) complex, with a paullone-based ligand, exchanges a chlorido ligand for an aqua ligand, within 72 h, only half as much as its ruthenium analogue, but thereby almost immediately reacting further to the hydroxo complex. The ruthenium analogue will exchange a chlorido ligand for an aqua ligand much faster, but the aqua complex shows no further sign of deprotonation.[55]

4. Cyclin-Dependent Kinases (CDKs) and Their Inhibitors

In the last years, research on CDKs, their regulators and substrates has been carried out in order to understand the regulation of the mammalian cell cycle.[58] The principles of the mode of action of CDKs are outlined in Chapter 2. For a better understanding of the role of CDK inhibitors, further detail will be given below.

Cyclins are produced at certain phases of the cell cycle. They periodically appear at the same stages of consecutive cycles. In addition, to the central role CDKs play in the cell cycle progression, members of this protein family have been associated with other potential roles. One of these roles is thought to be a CDK-regulating function, performed by the group of CDK-activating kinases (CAKs).[59] CAKs control the activity of CDKs by phosphorylation of specific Ser and Thr residues, needed for proper functioning. Additionally, several CAKs are able to phosphorylate the C-terminal domain of RNA polymerase II and thus control the transcription of cell cycle progression propagating proteins.[60]

4.1 The Role of Different CDKs in Cell Cycle Regulation

As mentioned before, progression through G1 phase is controlled by CDK4, CDK6 and the corresponding cyclin regulators. Quite recently, the additional contribution of CDK2 has been also elucidated.[9,61] At the beginning, mitogens (proteins, activating signal transduction pathways) initiate synthesis of D-type cyclins and probably regulate the required folding and channelling of CDK4 and/or CDK6 into the cell nucleus as well. The active complexes target members of the retinoblastoma (Rb) protein family (e.g. pRb) and accomplish phosphorylation. The members of the Rb family possess multiple phosphorylation sites for CDKs (e.g. 16 in pRb), but only some of them are recognized by CDK4-cyclinD and/or CDK6-cyclinD complexes.[58,62] As already outlined before, phosphorylation of pRb leads to the expression of E2F transcription factor.[63] Furthermore Rb proteins and E2F form active complexes, whose role is the enhancement of E-type cyclin expression, which are thought to be the activators of CDK2. The latter regulates the completion of G1 phase and is presumably responsible for the final degradation of CDK2-cyclinE as well. From this point in G1 onwards (‘restriction point’), the cells are believed to become independent of mito-

genic signals and cell division is continued without these stimuli.[9] Furthermore CDK2-cyclinE is thought to be essential for initiation of DNA replication, but as soon as the cell enters S phase, the enzyme needs to be deactivated. This is realised by degradation of cyclin E by an enzyme from the family of ubiquitin ligases and the subsequent segmentation by the proteasome.[64] The liberated CDK2 is bound to A- and B-type cyclins facilitating S phase transition. At the end of S phase, CDK2-cyclinA complexes are joined by CDK1-cyclinA complexes. The specific roles of these two species concerning S-G2 transition remains unclear.[58] However, it is known that on the one hand cyclinA is degraded during G2 and cyclinB is synthesised instead. On the other hand CDK1-cyclinB complexes enhance G2-M transition and progression through cell division.[65] Additionally, these enzyme complexes promote centrosome separation and are involved, for instance, in chromosomal condensation and breakdown of the nuclear lamina. Finally, the cell cycle comes to its end. To ensure that the exit from mitosis is performed accurately, CDK1-cyclinB complexes are degraded via ubiquitination by the anaphase-promoting complex (proteolytic pathway).[58,66]

4.2 CDK Inhibitors

Determination of primary, secondary and ternary structures[67] of CDKs has contributed primarily to the synthesis of the first inhibitors of these enzymes. First of all, it was found[68] that there are differences between the ternary structures of CDK2 in association with ATP[69] and the complex formed by CDK2, cyclin and ATP,[70] thus providing information about the conformational changes of the species on their association into the active complex. The influence of the natural inhibitors of CDKs on the conformation of the enzyme was also investigated. Furthermore the structures of p21 and $p19^{INK4d}$ could be established by X-ray diffraction[71] or NMR spectroscopy, respectively.[72] The protein p19 was also co-crystallised with CDK6. Thereby the active centre of the complex was located in the catalytic cleft between the two domains.[73] From these structural information three major approaches to the inhibition of CDKs were derived:

- Competitive inhibitors to ATP,
- Non-competitive inhibitors which use the same binding site as the natural ones,
- Molecules utilising both ways.

The first synthetic attempts took into account similarities of already known inhibitors of related protein kinases (Fig. 11), e.g. SU5416 (Semaxanib, (3Z)-3-[(3,5-dimethyl-1H-pyrrol-2-yl)methylidene]-1,3-dihydro-2H-indol-2-one; 12) which is a more advanced tyrosine kinase inhibitor. In further experiments some already well known drugs, such as the protein kinase C (PKC) inhibitor Staurosporine ((9S,10R,11R,13R)-2,3,10,11,12,13-Hexahydro-10-methoxy-9-methyl-11-(methylamino)-9,13-epoxy-1H,9H-diindolo[1,2,3-gh:3',2',1'-lm]pyrrolo[3,4-j][1,7]benzodiazonin-1-one; 13) showed significant CDK inhibition potential.[74-76]

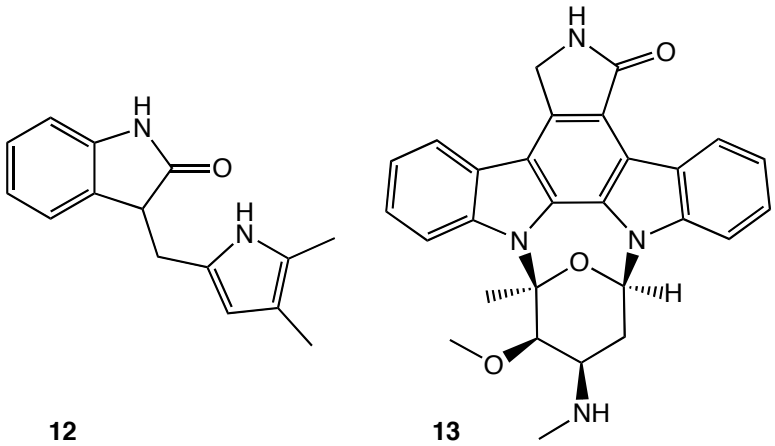

12 **13**

Figure 11. SU5416, (3Z)-3-[(3,5-dimethyl-1H-pyrrol-2-yl)methylidene]-1,3-dihydro-2H-indol-2-one (**12**); Staurosporine, (9S,10R,11R,13R)-2,3,10,11,12,13-Hexahydro-10-methoxy-9-methyl-11(methylamino)-9,13-epoxy-1H,9H-diindolo[1,2,3-gh:3',2',1'-lm]pyrrolo[3,4-j][1,7]benzodiazonin-1-one (**13**)

From the group of flavonoids, e.g. flavopiridol (2-(2-chlorophenyl)-5,7-dihydroxy-8-((3R,4S)-3-hydroxy-1-methylpiperidin-4-yl)-chromen-4-one, 14, Fig. 12), a non selective kinase inhibitor, exhibits noteworthy antiproliferative activity against CDKs in vitro.[77-80] The flavone core is the structural template, which is expanded by a piperidine unit in position 8 and an aryl substitution in position 2. By *in vivo* testing in mice, selective apoptosis of cells in the lymph nodes, the spleen and the thymus was observed, when administered daily as an intra venous bolus.[81]

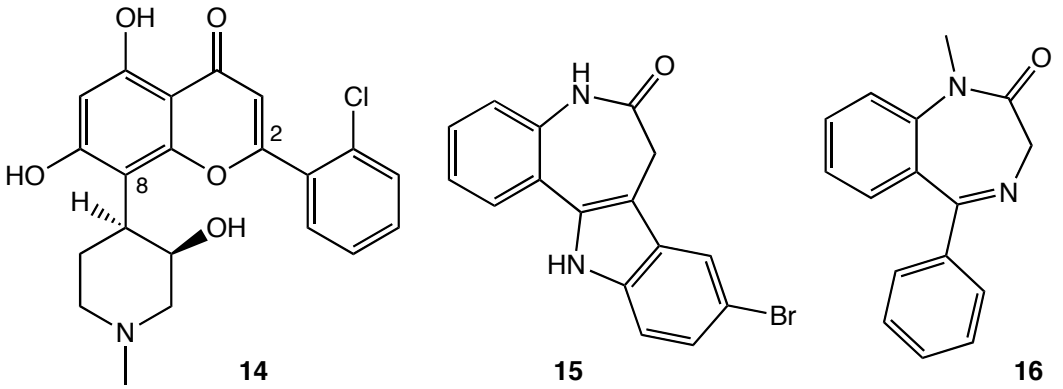

Figure 12. Flavopiridol, 2-(2-chlorophenyl)-5,7-dihydroxy-8-((3R,4S)-3-hydroxy-1-methylpiperidin-4-yl)-chromen-4-one (**14**); Kenpaullone, 9-Bromo-7,12-dihydroindolo[3,2-*d*][1]benzazepine (**15**); Valium® (**16**).

Paullones exhibit an activity profile similar to that of flavopiridol. The leading compound, 9-bromo-7,12-dihydroindolo[3,2-*d*][1]benzazepine (Kenpaullone; 15, Fig. 12), was found to be an inhibitor of CDK1-cyclinB and CDK2-cyclinE complexes.[82] The first successful synthesis of paullones was described in 1991.[83] Thereby benzazepine carboxylic acid esters were decarboxylated upon heating in DMF, with formation of 3,4-dihydro-1H-benz[b]azepine-2,5-dione. This underwent Fischer indol synthesis, yielding 7,12-dihydroindolo[3,2-*d*][1]benzazepine or its 9-bromo-substituted analogue kenpaullone (Fig. 13). Primarily the aim of paullone development was the improvement of already approved structural analogues, e.g. diazepam (Valium ®; 16, Fig. 12).

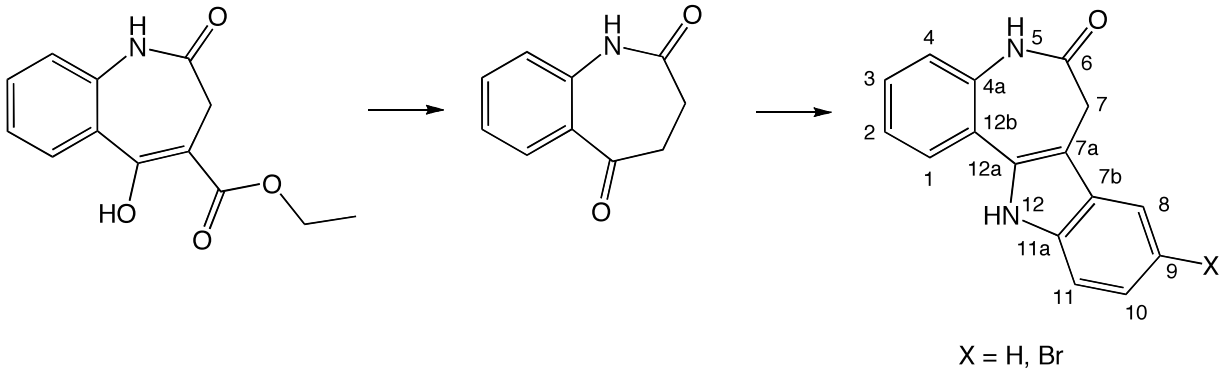

Figure 13. Synthesis of (the first) paullones.

The benzazepine dione was tested for its antiproliferative activity.[85,86] Paullones were also screened for antineoplastic properties in sixty human tumour cell lines at the NCI. This family of compounds is named after the designer of the screening algorithm (COMPARE), Kenneth Paull.[87]

Further structure-activity studies showed that the lactam unit of the azepine ring is essential for CDK inhibition, due to steric reasons.[88] Nonetheless other intracellular targets could be identified as well, e.g. glycogen synthase kinase 3β (GSK-3β)[89-91] and sirtuins.[92,93] The first inhibits GSK by phosphorylation and plays a role in cell cycle control as well. The second appears to be a regulator of p53 and associated with ageing and pathogenesis of viral and cancerous diseases. Especially substitution at the lactam unit seems to enhance the inhibiting properties of paullones towards sirtuins.

The poor solubility of paullones in aqueous and biological media remains a hurdle to be overcome. Therefore many derivatives have been synthesised in order to increase water solubility and anitproliferative activity as well. A promising approach is the derivatisation of the indolo benzazepine core structure, thus forming chelating binding sites for metal ions. Several complexes of paullone-based ligands to different metal ions are displayed in Fig. 14.

To perform modifications at the lactam unit, the latter must be activated first. Therefore the oxygen in position 6 is exchanged with sulfur by thionation, yielding the appropriate thio-lactam, which can be further derivatised with amines. To preserve the lactam unit, other ligands, with binding sites originating from paullone carbon C9, have been synthesised too. All these synthetic approaches are well known in the literature and some of them are described in the General Part.

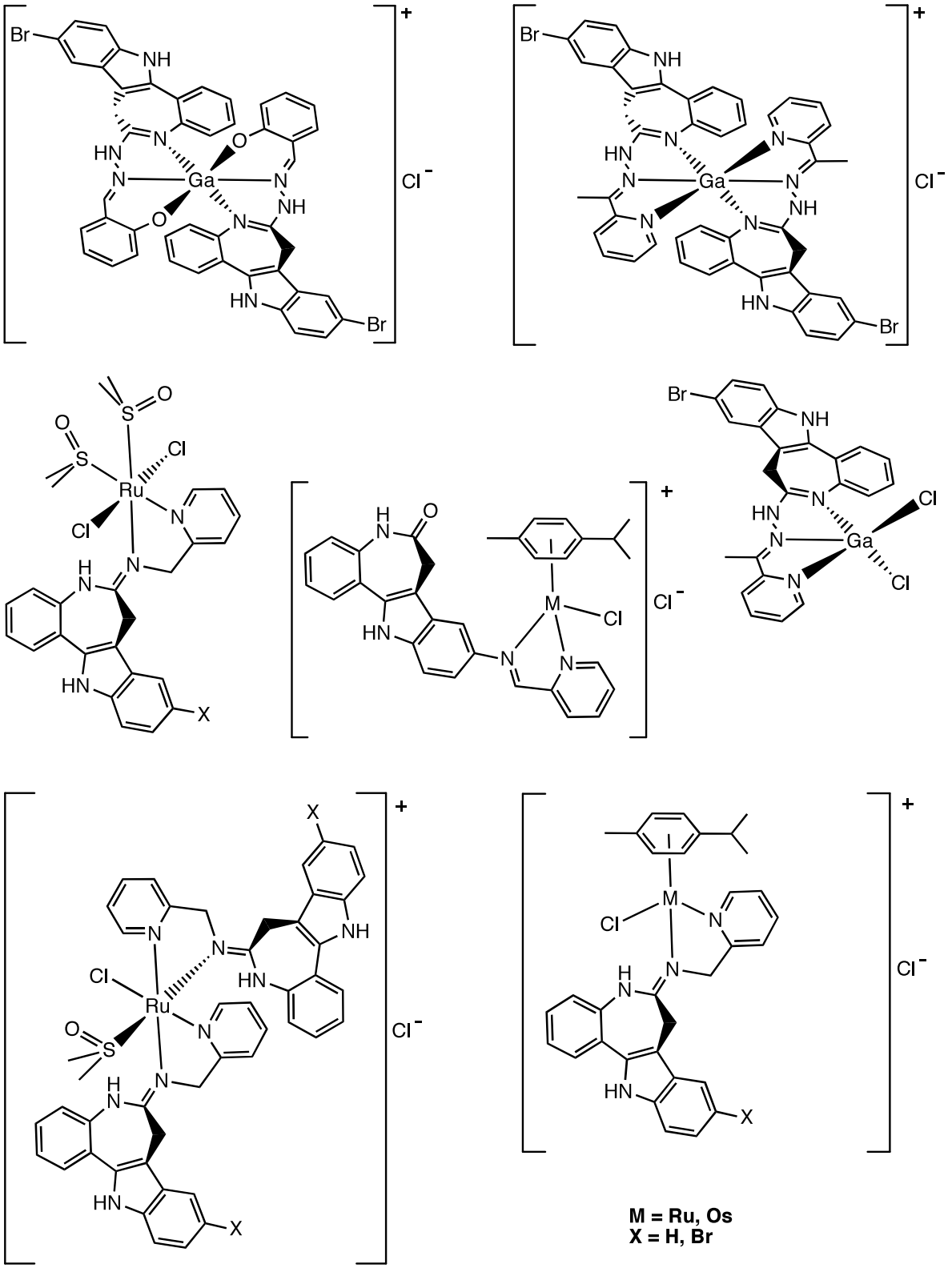

Figure 14. Paullone-based complexes of Ga^{3+}, Ru^{2+} and Os^{2+} developed throughout the last decade.

The development of gallium complexes is no longer followed because the problems with their solubility in aqueous media and stability could not be overcome. Complexes of ruthenium and osmium are still under development.

5. Copper

Copper is an element of the first group of transition metals. Along with silver and gold it belongs to the coin metals, a name which is derived from the ability of these metals to resist to corrosion. The name copper is derived from Latin “aes cyprium”, which can be translated as “ore of Cyprus”, as mines on Cyprus were exploited already in ancient times. About 3000 b.c. the advantageous properties of the binary alloy of copper and tin was discovered, consequently naming the upcoming age after the alloy – the Bronze Age.[42]

The natural isotopes of copper, namely ^{63}Cu and ^{65}Cu, make it accessible to NMR spectroscopy methods. Its electronic configuration is $[Ar]3d^{10}4s^{1}$, its preferred oxidation states are +1 (d^{10}, diamagnetic) and +2 (d^{9}, paramagnetic).[42]

Salts of copper(I) disproportionate in aqueous solutions to copper(II) and copper, due to the much higher hydration energy of the copper(II) ion. Consequently, only compounds of copper(I) which are insoluble or stable as complexes, do not undergo disproportionation. Differing from $[Cu(H_2O)_4]^{+}$, which disproportionates into Cu and $[Cu(H_2O)_6]^{2+}$, $[Cu(NH_3)_2]^{+}$ is a linear and stable ion, originating from the comproportionation of Cu and $[Cu(NH_3)_6]^{2+}$. In solution with concentrated ammonia, copper(I) forms the complex ion $[Cu(NH_3)_4]^{+}$, with tetrahedral geometry, as well. In contrast to copper(II), which prefers an octahedral coordination sphere in crystals and complexes as well, copper(I) is more likely to be found in tetrahedral geometry. Copper(II) complexes are a subject of the so-called Jahn-Teller effect. This theorem describes an electronic effect, which appears in non-linear molecules with a degenerated electronic ground state, yielding a geometrical distortion of the coordination polyhedron, thus resulting in a removal of degeneracy and a decrease of the overall energy of the complex. As a consequence, several copper(II) complexes are additionally coordinated by two aqua ligands in the axial positions above and below the square plane of coordination: $[Cu(H_2O)_6]^{2+}$, $[Cu(NH_3)_4(H_2O)_2]^{2+}$. In crystals of copper(II) compounds the distortion can be found preferentially as a elongation and rarely as a compression of the octahedron. It should be mentioned as well, that copper(II) compounds are, due to the d^{9} electronic state, brightly coloured, whereas copper(I) compounds are usually colourless. The potential difference, between these two oxidation states, make copper a valuable metal for redox processes occurring in biological systems.[42]

5.1 Copper in Biological Systems

For most aerobic organisms copper is an essential trace element. An average adult male contains about 100 mg of the metal.[94] It serves as a catalytic and structural co-factor for enzymes involved in energy production, oxygen transport, cellular metabolism, signal transduction, blood clotting and many other processes.[95] In molluscs and crabs the copper containing protein haemocyanin is responsible for the transport of oxygen.[42] As mentioned before, under physiological conditions, copper can exist in its oxidation states Cu^{+} and Cu^{2+}. Each ion is distinct from the other by its specific coordination chemistry. The fully occupied d-orbitals of Cu^{+} (d^{10}) make it a "softer" ion according to the HSAB principle, whereas Cu^{2+} is a "harder" coordination centre compared to Cu^{+}. Thus Cu^{+} prefers "softer" ligands (e.g. sulfur donors), and Cu^{2+} is more likely to bind with "harder" ligands (nitrogen or oxygen donors), respectively. Thus proteins coordinated to Cu^{+} preferentially bind via sulfur containing amino acid side chains of cysteine or methionine, whereas Cu^{2+} more likely bound through the nitrogen or oxygen bearing amino acid side chains of histidine (N) or glutamate (O) or aspartate (O).[96,97] As a result copper is facilitating an unexpectedly high number of biological processes. One of the most prominent representatives of the group of metal-based enzymes: the Cu/Zn superoxide dismutase (SOD1, Fig. 15), which catalyzes the disproportionation reaction of metabolic side product superoxide into dioxygen or into hydrogen peroxide if the milieu is acidic. Thereby Cu^{2+} gets reduced to Cu^{+}. It should be mentioned in this context, that it is of central importance to biological systems to possess a functioning system for metal ion absorption and distribution to the appropriate targets, as otherwise free metal ions are likely to exhibit their redox activity in places unwanted. Thus they are likely to undergo Fenton type reactions with hydrogen peroxide, yielding even more reactive oxygen species. Other defects in the homeostasis of copper are directly correlated with human diseases. For example, mutations in the P-type ATPases ATP7A and ATP7B (ATP driven Cu^{+} pumps), expressed in extrahepatic tissues or in the liver, respectively, are responsible for the occurrence of Menkes and Wilson's disease.[95]

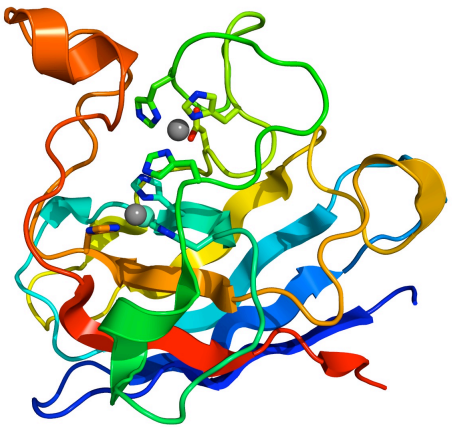

Figure 15. Structure of human Cu/Zn SOD.[98]

In eukaryotic cells, copper acquisition is enhanced by the integral membrane protein Ctr1. The protein consists of three transmembrane domains. Three proteins associate as a homotrimer, likely to form a pore for copper import.[99-102] The structure of Ctr1 is structurally and functionally conserved from yeast to humans.[103-105] The results of further research strongly suggest, that the pore is highly affine to Cu^{+}, as Ctr1 only reaches its maximal activity in the presence of cell surface Cu^{2+}/Fe^{3+} metalloreductase Fre1 and Fre2,[106] but it remains yet unclear how Cu^{+} is preserved in its oxidation state in the presence of oxygen before Ctr1 mediated import. Ctr1 plays a role in intracellular mobilisation of copper storages as well. Additional transporters e.g. Ctr2 or Ctr6 could be identified in *S.cervisieae* (baker's yeast) or *S.pombe* (fission yeast), respectively.[106-109] On the one hand the details of transport are still topic of discussions,[95] but on the other hand copper transport to mitochondria and integration into cytochrome *c* oxidase (Fig. 16) has been studied excessively.[111]

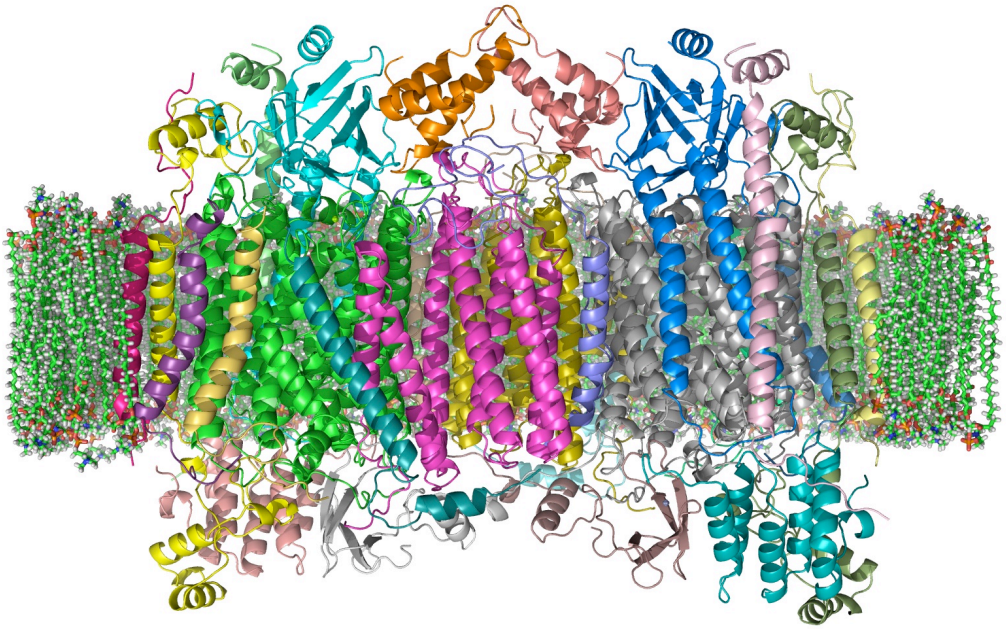

Figure 16. Structure of human cytochrome c peroxidase.

The chaperone protein Cox17 appears to be the protagonist, responsible for cytochrome *c* oxidase assembly. The latter is a key enzyme of the mitochondrial respiratory chain, the final step in the main way of energy generation in aerobic cells. Involved in this important process of cellular life, copper became a popular target for drugs, as well as a mediator of drugs, being a centre of coordination.

In conjunction with the topic of this thesis, especially the role of copper compounds in cancer therapy will be dealt with.

5.2 Copper in Cancer Treatment

In relation with cancer, many clinical trials have shown that the concentration of copper is elevated in the serum, as well as in the tumour.[112] Furthermore copper is thought to be another stimulating factor of angiogenesis (next to other growth factors).[113-115] Consequently, copper is required for uncontrolled proliferation of malignant neoplasms.

One approach to cancer treatment through copper is the administration of copper chelating ligands, e.g. D-penicillamine (D-pen).[112] This possible drug benefits from the elevated level of oxidative stress in tumours. As it reduces Cu^{2+}, yielding Cu^{+} and a D-pen radical it contributes to the formation of ROS. The formed Cu^{+} does the same, as its oxidation back to Cu^{2+} yields a superoxide anion. Thus the oxidative stress is increased continuously, finally reaching a lethal level, leading the cancer cell to apoptosis.

A second approach is the same as described for gallium(III) and ruthenium(III). The excessive need of tumours for nutrients leads to a higher acquisition of metal ions, compared to normal cells. As the same is true for copper, copper chelators have been of frequent interest as potential anti-tumour drugs. Up to present day many compounds have been tested. Several well-known bis(thiosemicarbazones) and their copper(II) complexes show encouraging anti-tumor activity, which has been demonstrated by both *in vitro* and *in vivo* experiments,[116-117] as well as copper(II) complexes of purine derivatives, benzohydroxamic acid, imidazole derivatives and polycarboxylates have been synthesised, characterised and tested for cytotoxicity.[57]

References

[1] According to http://www.who.int/cancer/en/ (2009-08-09).

[2] According to Statistik Austria, *Gestorbene in Österreich ab 1970 nach Todesursachen und Geschlecht*, **2009**, http://www.statistik.at/web_de/statistiken/gesundheit/todesursachen/todesursachen_im_ueberblick/index.html (2009-09-27).

[3] According to Statistik Austria, *Malignome, insgesamt (C00–C43, C45–C99) - Krebsmortalität (Sterbefälle pro Jahr), Österreich ab 1983* **2009**, http://www.statistik.at/web_de/statistiken/gesundheit/krebserkrankungen/malignome_insgesamt/index.html (2009-09-27).

[4] Hanahan, D.; Weinberg, R. A. *Cell* **2000**, *7*, 57–70.

[5] Löffler, G.; Petrides, P. E.; Heinrich, P. C. *Biochemie & Pathobiochemie*, 8. Auflage 2007, Heidelberg, 220 pp.

[6] Alberts et. al. *Molecularbiology of the Cell*, Taylor & Francis, 4thEdition, **2002**.

[7] Knockaert, M.; Greengard, P., Meijer, L *Trends Pharmacol. Sci.*, **2002**, *23*, 9, 417–425.

[8] Soni, R.; O'Reilly, T.; Furet, P.; Muller, L.; Stephan, C.; Zumstein-Mecker, S.; Fretz, H; Fabbro, D.; Chaudhuri, B. *J. Natl. Cancer I.*, **2001**, *93*, 436–446.

[9] Malumbres, M.; Barbacid, M. *Nat. Rev. Cancer*, **2001**, *1*, 222–231.

[10] Cohen, P. *Nat. Rev. Drug Discovery*, **2002**, *1*, 309–315.

[11] According to http://www.whocc.no/atcddd/ (2009-09-14).

[12] Peyrone, M. *Ann. Chem. Pharm.* **1844**, *51*, 1–29.

[13] Rosenberg, B.; Van Camp, L.; Krigas, T. *Nature* **1965**, *205*, 698–699.

[14] Rosenberg, B.; Van Camp, L.; Grimley, E. B.; Thomson, A. J. *J. Biol. Chem.* **1967**, *242*, 1347–1352.

[15] Jakupec, M. A.; Galanski, M.; Keppler, B. K. *Rev. Physiol. Bioch. P.* **2006**, *146*, 1–53.

[16] Fichtinger-Schepman, A. M. J.; Van der Leer, J. L.; den Hartog, J. H. J.; Lohman, P. H. M.; Reedijk, J. *Biochemistry* **1985**, *24*, 707–713.

[17] Knox, R. J.; Friedlos, F.; Lydall, D. A.; Roberts, J. J. *Cancer Res.* **1986**, *46*, 1972–1979.

[18] Kidani, Y.; Inagaki, K.; Iigo, M.; Hoshi, A.; Kuretani, K. *J. Med. Chem.* **1978**, *21*, 1315–1318.

[19] Saris, C. P.; van der Vaart, P. J.; Rietbroek, R. C.; Blommert, F. A. *Carcinogenesis* **1996**, *17*, 2763–2769.

[20] Woynarowski, J. M.; Faivre, S.; Herzig, M. C. S.; Arnett, B.; Chapman, W. G.; Trevino, A. V.; Raymond, E.; Chaney, S. G.; Vaisman, A.; Varchenko, M.; Juniewicz, P. E. *Mol. Pharmacol.* **2000**, *58*, 920–927.

[21] According to http://www.gpcbiotech.com/en/news_media/press_releases/2007/07-30-2007.html (2009-09-17).

[22] Heffeter, P.; Jungwirth, U.; Jakupec, M.; Hartinger, C.; Galanski, M.; Elbling, L.; Micksche, M.; Keppler, B.; Berger, W. *Drug Resist. Update* **2008**, *11*, 1–16.

[23] Galanski, M.; Arion, V. B.; Jakupec, M. A.; Keppler, B. K. *Curr. Pharm. Design* **2003**, *9*, 2078–2089.

[24] Jakupec, M. A.; Galanski, M.; Arion, V. B.; Hartinger, C. G.; Keppler, B. K. *Dalton Trans.* **2008**, *2*, 183–194.

[25] Dudley, H. C.; Imirie, G. W. Jr.; Istock, J. T. *Radiology* **1950**, *55*, 571–578.

[26] Edwards, C. L.; Hayes, R. L. *J. Nucl. Med.* **1969**, *10*, 103–105.

[27] Edwards, C. L.; Hayes, R. L. *J. Amer. Med. Ass.* **1970**, *212*, 1182–1190.

[28] Welin, M., Moche, M., Arrowsmith, C. H., Berglund, H., Busam, R. D., Collins, R., Dahlgren, L. G., Edwards, A. M., Flodin, S., Flores, A., Graslund, S., Hammarstrom, M., Herman, M. D., Johansson, A., Johansson, I., Kallas, A., Karlberg, T., Kotenyova, T., Lehtio, L., Nilsson, M. E., Nyman, T., Persson, C., Sagemark, J., Schueler, H., Svensson, L., Thorsell, A. G., Tresaugues, L., Van Den Berg, S., Weigelt, J., Wikstrom, M., Nordlund, P *to be published* Image derived from the RCSB PDB, DOI:10.2210/pdb2vux/pdb, available at http://www.rcsb.org/pdb/explore.do?structureId=2VUX (2009-09-20).

[29] Chitambar, C. R. *Curr. Opin. Oncol.* **2004**, *16*, 547–552.

[30] Bedikian, A. Y; Valdivieso, M.; Bodey, G. P.; Burgess, M. A.; Benjamin, R. S.; Hall, S.; Freireich E. J. *Cancer Treat. Rep.* **1978**, *62*, 1449–1453.

[31] Samson, M. K.; Fraile, R. J.; Baker, L. H.; O'Bryan, R. *Cancer Clin. Trials* **1980**, *3*, 181–186.

[32] Seidman, A. D., Scher, H. I., Heinemann, M. H.; Bajorin, D. F.; Sternberg, C. N.; Dershaw, D. D.; Silverberg, M.; Bosl, G. J. *Cancer* **1991**, *68*, 2561–2565.

[33] Collery, P.; Keppler, B.; Madoulet, C.; Desoize. B. *Crit. Rev. Oncol. Hemat.* **2002**, *42*, 283–296.

[34] Jakupec, M. A.; Keppler, B. K. *Curr. Top. Med. Chem.* **2004**, *4*, 1575–1583.

[35] Lum, B. L.; Srivanas, S.; Beck, J. T.; Vesole, D.; Largey, M.; Valone, F. H.; Sayre, P. H. *Proc. Am. Soc. Clin. Oncol.* **2003**, *22*, abstr. 943.

[36] Hofheinz, R. D.; Dittrich, C.; Jakupec, M. A.; Drescher, A.; Jaehde, U.; Gneist, M.; et al. Int. *J. Clin. Pharm. Ther.* **2005**, *43*, 590–591.

[37] Bernstein, L. R.; Tanner, T.; Godfrey, C.; Noll, B. *Met.-Based Drugs* **2000**, *7*, 33–47.

[38] Collery, P.; Millhart, H.; Pechery, C.; Kratz, F.; Keppler, B. K. in Metal Ions in Biology and Medicine; Vol. 2; Anastassopoulou, J.; Collery, P.; Etienne, J. C.; Theophanides, T.; Eds.; Libbey Eurotext: Paris, 1992, pp 173–175.

[39] Collery, P.; Domingo, J. L.; Keppler, B. K. *Anticancer Res.* **1996**, *16*, 687–692.

[40] Dobrov, A.; Arion, V. B.; Kandler, N.; Ginzinger, W.; Jakupec, M. A.; Rufiska, A.; Graf von Keyserlingk, N.; Galanski, M.; Kowol, C.; Keppler, B. K. *Inorg. Chem.* **2006**, 45, 1945–1950.

[41] Ginzinger, W.; Arion, V. B.; Giester, G.; Galanski, M.; Keppler, B. K. *Cent. Eur. J. Chem.* **2008**, *6*, 340–346.

[42] Holleman, A. F.; Wiberg, E. Lehrbuch der Anorganischen Chemie; Berlin, New York, 1995.

[43] Rademaker-Lakhai, J. M.; van den Bongard, D.; Pluim, D.; Beijnen, J. H.; Schellens, J. H. M. *Clin. Cancer Res.* **2004**, *10*, 3717–3727.

[44] Dittrich, C.; Scheulen, M. E.; Jaehde, U.; Kynast, B.; Gneist, M; Richly, H.; Schaad, S.; Arion, V. B.; Keppler, B. K. *P. Am. Assoc. Cancer Res.* **2005**, *46*, P472.

[45] Hartinger, C. G.; Jakupec, M. A.; Zorbas-Seifried, S.; Groessl, M.; Egger, A.; Berger, W.; Zorbas, H.; Dyson, P. J.; Keppler, B. K. *Chem. Biodivers.* **2008**, *5*, 2140–2155.

[46] Lentz, F.; Drescher, A.; Lindauer, A.; Henke, M.; Hilger, R. A.; Hartinger, C. G.; Scheulen, M. E.; Dittrich, C.; Keppler, B. K.; Jaehde, U. *Anti-Cancer Drug*, **2009**, *20*, 97–103.

[47] Clarke, M. J. in *Metal Ions in Biological Systems*, ed. H. Sigel, M. Dekker, Basel, 1980, voll. 11, p. 231.

[48] Gianferrara, T.; Bratsos, I.; Alessio, E. *Dalton Trans.*, **2009**, 7588–7598.

[49] Gatenby, R. A.; Gillies, R. J. *Nat. Rev. Cancer* **2004**, *4*, 891–899.

[50] Chen, H.; Parkinson, J. A.; Morris, R. E.; Sadler, P. J. *J. Am. Chem. Soc.* **2003**, *125*, 173–186.

[51] Dyson, P. J. *Chimia* **2007**, *61*, 698–703.

[52] Habtemariam, A.; Melchart, M.; Fernández, R.; Parsons, S.; Oswald, I. D. H.; Parkin, A.; Fabbiani, F. P. A.; Davidson, J. E.; Aird, R. E.; Jodrell, D. I.; Sadler, P. J. *J. Med. Chem.* **2006**, *49*, 6858–6868.

[53] Schmid, W. F.; Zorbas-Seifried, S.; John, R. O.; Arion,V. B.; Jakupec, M. A.; Roller, A.; Galanski, M.; Chiorescu, I.; Zorbas, H.; Keppler B. K. *Inorg. Chem.* **2007**, *46*, 3645–3656.

[54] Schmid, W. F.; John, R. O.; Arion, V. B.; Jakupec, M. A.; Keppler B. K. *Organometallics*, **2007,** *26*, 6643–6652.

[55] Schmid, W. F.; John, R. O.; Mühlgassner, G.; Heffeter, P.; Jakupec, M. A.; Galanski, M.; Berger, W.; Arion, V. B.; Keppler, B. K. *J. Med. Chem.* **2007,** *50,* 6343–6355.

[56] Peacock, A. F. A.; Melchart, M.; Deeth, R. J.; Habtemariam, A.; Parsons, S.; Sadler, P. J. *Chem. Eur. J.* **2007**, *13*, 2601–2613.

[57] Gielen, M.; Tieknik, E. R. T. *Metallotherapeutic Drugs and Metal-Based Diagnostic Agents: The Use of Metals in Medicine*, **2005**, Wiley & Sons, Ltd., Chichester, England.

[58] Malumbres, M.; Barbacid, M. *Trends Biochem. Sci.* **2005**, *30*, 630–641.

[59] Kaldis, P. *Cell. Mol. Life Sci.* **1999**, *55*, 284–296.

[60] Fisher, R. P.; Morgan, D. O. *Biochim. Biophys. Acta* **1996**, *1288*, 7–10.

[61] Sherr, C. J.; Roberts, J. M. *Gene Dev.* **1999**, *13*, 1501–1512.

[62] Cobrinik, D. *Oncogene* **2005**, *24*, 2796–2809.

[63] Murray, A. *Chem. Biol.* **1994**, *1*, 191–195.

[64] Hwang, H. C.; Clurman, B. E. *Oncogene* **2005**, *24*, 2776–2786.

[65] Nigg, E. A. *Nat. Rev. Mol. Cell Biol.* **2001**, *2*, 21–32.

[66] Harper, J. W.; Burton, J. L.; Solomon, M. J. *Gene Dev.* **2002**, *16*, 2179–2206.

[67] Morgan, D. O. *Curr. Opin. Cell Biol.* **1996**, *8*, 767–772.

[68] Kim, S.-H. *Pure Appl. Chem.* **1998**, *70*, 555–565.

[69] De Bondt, H. L.; Rosenblatt, J.; Jancarik, J.; Jones, H. D.; Morgan, D. O.; Kim, S.-H. *Nature* **1993**, *363*, 595–602.

[70] Jeffrey, P. D.; Russo, A. A.; Polyak, K.; Gibbs, E.; Hurwitz, J.; Massague, J.; Pavletich, N. P. *Nature* **1995**, *376*, 313–320.

[71] Mayrose, D. R.; Nichols, M. A.; Xiong, Y.; Ke, H. *Protein Sci.* **1996**, *5*, 1928–1930.

[72] Luh, F. Y.; Archer, S. J.; Domaille, P. J.; Smith, B. O.; Owen, D.; Brotherton, D. H.; Raine, A. R. C.; Xu, X.; Brizuela, L.; Brenner, S.; Laue, E. D. *Nature* **1997**, *389*, 999–1003.

[73] Brotherton, D. H.; Dhanaraj, V.; Wick, S.; Brizuela, L.; Domaille, P. J.; Volyanik, E.; Xu, X.; Parisini, E.; Smith, B. O.; Archer, S.; Serrano, M.; Brenner, S.; Blundell, T. L.; Laue, E. D. *Nature* **1998**, *395*, 244–250.

[74] Meijer, L. *Trends Cell. Biol.* **1996**, *6*, 393–397.

[75] Gadbois, D.; Hamaguchi, J. R.; Swank, R. A.; Bradbury, E. M. *Biochem. Bioph. Res. Co.* **1992**, *184*, 80–85.

[76] Meijer, L. in *Progress in Cell Cycle Research*; Plenum Press: New York, 1995: Vol.1, pp 351–361.

[77] NCI PDG Clinical Trial Search, November 1997 - http://www.cancer.gov/clinicaltrials/.

[78] R&D Drug news **1998**, Jan. 19.

[79] Senderowicz, A. M.; Headlee, D.; Stinson, S. F.; Lush, R. M.; Kalil, N.; Villalba, L.; Hill, K.; Steinberg, S. M.; Figg, W. D.; Tompkins, A.; Arbuck, S. G.; Sausville, E. A. *J. Clin. Oncol.* **1998**, *16*, 2986–2999.

[80] Mansuri, M. M.; Murthi, K. K.; Pal, K. PCT Int. Apl. WO 9716447 A1 970509.

[81] Arguello, F.; Alexander, M.; Sterry, J. A.; Tudor, G.; Smith, E. M.; Kalavar, N. T.; Greene, J. F. Jr.; Koss, W.; Morgan, C. D.; Stinson, S. F.; Siford, T. J.; Alvord, G.; Klabansky, R. L.; Sausville, E. A. *Blood* **1998**, *91*, 2482–2490.

[82] Zaharevitz, D.; Kunick, C.; Schultz, C.; Meijer, L.; Leost, M.; Gussio, R.; Senderowicz, A.; Lahusen, T.; Sausville, E. *Am. Assoc. Cancer Res.* **1999**, *Apr. 10–14*.

[83] Kunick, C. *Arch. Pharm. (Weinheim, Ger.)* **1991**, *324*, 579–581.

[84] Kunick, C. *Arch. Pharm. (Weinheim, Ger.)* **1992**, *325*, 297–299.

[85] Rees, A. H. *J. Chem. Soc.* **1959**, 3111–3116.

[86] Rees, A. H.; James, D. M. *J. Med. Pharm. Chem.* **1962**, *5*, 1234–1238.

[87] Paull, K. D.; Shoemaker, R. H.; Hodes, L.; Monks, A.; Scudiero, D. A.; Rubinstein, L.; Plowman, J.; Boyd, M. R. *J. Natl. Cancer I.* **1989**, *81*, 1088–1092.

[88] Schultz, C.; Link, A.; Leost, M.; Zaharewitz, D. W.; Gussio, R.; Sausville, E. A.; Meijer, L.; Kunick, C. *J. Med. Chem.* **1999**, *42*, 2909–2919.

[89] Leost, M.; Schultz, C.; Link, A.; Wu, Y.-Z.; Biernat, J.; Mandelkow, E.-M.; Bibb, J. A.; Snyder, G. L.; Greengard, P.; Zaharewitz, D. W.; Gussio, R.; Senderowicz, A. M.; Sausville, E. A.; Kunick, C.; Meijer, L. *Eur. J. Biochem.* **2000**, *267*, 5983–5994.

[90] Kunick, C.; Lauenroth, K.; Wieking, K.; Xie, X.; Schultz, C.; Gussio, R.; Zaharewitz, D.; Leost, M.; Meijer, L.; Weber, A.; Jorgensen, F. S.; Lemcke, T. *J. Med. Chem.* **2004**, *47*, 22–36.

[91] Zhu, L.; Hou, T.; Xu, X. *J. Mol. Model.* **2001**, *7*, 223–230.

[92] Vaziri, H.; Dessain, S. K.; Eaton, E.; Imai, S. I. ; Frye, R. A. et al. *Cell* **2001**, *107*, 149–159.

[93] Trapp, J.; Jochum, A.; Meier, R.; Saunders, L.; Marshall, B.; Kunick, C.; Verdin, E.; Goekjian, P.; Sippl, W.; Jung, M. *J. Med. Chem.* **2006**, *49*, 7307–7316.

[94] Linder, M. C.; Goode, C. A. *Biochemistry of Copper* 1-413 (Springer, New York, 1991).

[95] Kim, B.-E.; Nevitt, T.; Thiele, D. J. *Nat. Chem. Biol.* **2008**, *4*, 176–185.

[96] Bertini, I.; Gray, H. B.; Stiefel, E.; Valentine, J.S. *Biological Inorganic Chemistry* (Sausalito, CA, USA, 2007).

[97] Lippard, S. J.; Berg, J. M. *Principles of Bioinorganic Chemistry*, 3-388 (University Science Books, Mill Valley, CA, USA, 1994).

[98] Cao, X.; Antonyuk, S. V.; Seetharaman, S. V.; Whitson, L. J.; Taylor, A. B.; Holloway, S. P.; Strange, R. W.; Doucette, P. A.; Valentine, J. S.; Tiwari, A.; Hayward, L. J.; Padua, S.; Cohlberg, J. A.; Hasnain, S. S.; Hart, P. J. *J. Biol. Chem.* **2008**, *283*, 16169–16177

[99] Nose, Y.; Kim, B. E.; Thiele, D. J. *Cell Metab.* **2006**, *4*, 235–244.

[100] Dancis, A. et al. *Cell* **1994**, *76*, 393–402.

[101] Pena, M. M.; Puig, S.; Thiele, D. J. *J. Biol. Chem.* **2000**, *275*, 33244–33251.

[102] Aller, S. G.; Unger, V. M. *Proc. Natl. Acad. Sci. USA* **2006**, *103*, 3627–3632.

[103] Nose, Y.; Rees, E. M.; Thiele, D. J. *Trends Biochem. Sci.* **2006**, *31*, 604–607.

[104] Puig, S.; Thiele, D. J. *Curr. Opin. Chem. Biol.* **2002**, *6*, 171–180.

[105] Maryon, E. B.; Molloy, S. A.; Zimnicka, A. M.; Kaplan, J. H. *Biometals* **2007**, *20*, 355–364.

[106] Rees, E. M.; Thiele, D. J. *J. Biol. Chem.* **2007**, *282*, 21629–21638.

[107] Portnoy, M. E.; Schmidt, P. J.; Rogers, R. S.; Culotta, V. C. *Mol. Genet. Genomics* **2001**, *265*, 873–882.

[108] Rees, E. M.; Lee, J.; Thiele, D. J. *J. Biol. Chem.* **2004**, *279*, 54221–54229.

[109] Bellemare, D. R. et al *J. Biol. Chem.* **2002**, *277*, 46676–46686.

[110] Tsukihara, T.; Aoyama, H.; Yamashita, E.; Tomizaki, T.; Yamaguchi, H.; Shinzawa-Itoh, K.; Nakashima, R.; Yaono, R.; Yoshikawa, S. *Science* **1996**, *272*, 1136–1144.

[111] Cobine, P. A.; Ojeda, L. D.; Rigby, K. M.; Winge, D. R. *J. Biol. Chem.* **2004**, *279*, 14447–14455.

[112] Gupte, A.; Mumper, R. J. *Cancer Treat. Rev.* **2009**, *35*, 32–46.

[113] Folkman, J.; Klagsburn, M. *Science* **1987**, *235*, 442–447.

[114] Brewer, G. *Drug Dis. Today*, **2005**, *10*, 1103–1109.

[115] Brem, S. *Cancer Control*, **1999**, *6*, 436–458.

[116] Petering, D. H. *Metal Ions Biol. Syst.*, **1980**, *11*, 197–229.

[117] French, F. A.; Blanz Jr., E. J.; *Cancer Res.*, **1965**, *25*, 1454-1458; **1966**, *26*, 1638–1640.

General Part

Within this work novel complexes of copper(II) with paullone-based ligands have been synthesised, characterised and tested for antiproliferative activity *in vitro*. The results of these studies have been summarised in a paper submitted to *Inorganic Chemistry*. The manuscript submitted follows in the next section and is formatted according to the guidelines for authors of the journal.

Highly Cytotoxic Copper(II) Complexes with Modified Paullone Ligands

Michael F. Primik,[†] Gerhard Mühlgassner,[†] Michael A. Jakupec,[†] Olivier Zava,[‡]

Paul J. Dyson,[‡] Vladimir B. Arion,[†,*] Bernhard K. Keppler[†]

[†]*Institute of Inorganic Chemistry, University of Vienna, Währinger Str. 42, A-1090 Vienna, Austria, and* [‡]*Institut des Sciences et Ingénierie Chimiques, Ecole Polytechnique Fédérale de Lausanne (EPFL), CH-1015 Lausanne, Switzerland*

Antiproliferative Copper(II)-Paullone Complexes

*To whom correspondence should be addressed. Address: Institute of Inorganic Chemistry, University of Vienna, Währinger Str. 42, A-1090 Vienna, Austria. Phone: +431427752615. Fax: +431427752680. E-mail: vladimir.arion@univie.ac.at.

Abstract

The reaction of copper(II) chloride or copper(II) acetate with 6-N-(2-N′,N′-dimethylaminoethylamino)-7,12-dihydroindolo-[3,2-*d*][1]benzazepine (HL^1), 9-bromo-6-N-(2-N′,N′-dimethylaminoethylamino)-7,12-dihydroindolo-[3,2-*d*][1]benzazepine (HL^2), N-(9-bromo-7,12-dihydroindolo[3,2-*d*][1]benzazepin-6(5*H*)-yliden-N'-(1-pyridin-2-yl-methylidene)azine (HL^3) or N-(9-bromo-7,12-dihydroindolo[3,2-*d*][1]benzazepin-6(5*H*)-yliden-N'-(1-pyridin-2-yl-ethylidene)azine (HL^4) in methanol affords the novel copper(II) complexes $[Cu(HL^1)Cl_2]$ (**1**), $[Cu(HL^2)Cl_2]$ (**2**), $[Cu(HL^3)Cl_2]\cdot 1.5CH_3OH$ (**3**), $[Cu(HL^4)Cl_2]\cdot 1.5H_2O$ (**4**) and $[Cu(HL^4)(CH_3COO)(CH_3OH)]\cdot 3CH_3OH$ (**5**). The new ligands (HL^2 and HL^3) and the complexes **1**−**5** were characterized by ^{1}H NMR, ^{13}C NMR, IR and electronic absorption spectroscopy, ESI mass spectrometry and X-ray crystallography. Two ligands, HL^1 and HL^2, and complexes **1**−**4** were tested for cytotoxicity in three human cancer cell lines, namely CH1 (ovarian carcinoma), A549 (non-small cell lung cancer) and SW480 (colon carcinoma). Additionally, complexes **1, 2** and **4** were assayed in an isogenic pair of ovarian cancer cell lines, one being sensitive to cisplatin (A2780) and the other having acquired cisplatin resistance (A2780cisR). All of the compounds evaluated are cytotoxic, with complexes **3** and **4** exhibiting IC_{50} values in the nanomolar range.

Introduction

Many anticancer drugs used today are either classical non-targeted coordination complexes or organic intercalators, but they are increasingly used in combination with targeted organic compounds that inhibit specific enzymes. In recent years, efforts to construct hybrid drug systems in which a targeted organic drug is attached to a non-targeted metal center have emerged.[1] Indeed, metal complexes with biologically active ligands display many favourable properties that could overcome the limitations encountered in combination therapies.[2−13] In this regard, recent efforts by us have focussed on the synthesis of metal complexes with indolo[3,2-*d*]benzazepines (Paullones), which inhibit the activity of cyclin-dependent kinases (CDKs) and show high cytotoxicity in vitro.[14,15] Structure–activity relationship studies on metal-free compounds have revealed certain features required for CDK-inhibitory properties

that do not necessarily parallel their antiproliferative activity profile.[16] As a result, other intracellular targets for Paullones have also been suggested.[15,17] Our primary aim has been to investigate the effect of metallation of Paullone compounds on both CDK-inhibition and cytotoxicity. Since the original Paullone derivatives do not contain binding sites to accommodate metal ions, a number of novel indolo[3,2-*d*]benzazepines have been designed and synthesized and subsequently coordinated to gallium(III), ruthenium(II) and osmium(II) centers.[18–21] The effect of metal coordination on the aqueous solubility, antiproliferative activity and impact on the cell cycle has been reported.[18–21] As a natural extension to this work, we turned our attention to ligands that are able to bind copper(II), as a more biologically compatible metal ion.

Copper is an essential element for most aerobic organisms, employed as a structural and catalytic cofactor, and consequently it is involved in many biological pathways.[22–25] Taking this into account, much attention has been given to research on the mechanisms of absorption,[26–28] distribution,[29–31] metabolism and excretion of copper,[32–34] as well as on its role in the development of cancer and other diseases.[35,36] In the case of cancer, numerous studies have shown that the concentration of copper is elevated in the serum, as well as in the tumor,[24,37–51] as copper is an endogenous angiogenesis stimulator.[52–54] Nevertheless, several bis(thiosemicarbazones) and their copper(II) complexes show encouraging anti-tumor activity, which has been demonstrated *in vitro* and *in vivo*.[55,56] Moreover, a number of copper(II) complexes with purine-based, benzohydroxamic acid, imidazole and polycarboxylate ligands have been shown to exhibit good cytotoxicities.[57]

Herein we report on the synthesis of the first Paullone-based copper(II) complexes of the general formulae $[Cu(HL^{1–4})Cl_2]$ and $[Cu(L^4)(CH_3COO)(CH_3OH)]$, where HL^1 and HL^2 are bidentate ligands and HL^3 and HL^4 tridentate ligands (Scheme 1). Their spectroscopic properties, solid state structures, and cytotoxicity in human cancer cell lines are also reported.

Scheme 1. Synthesis of **1**−**5** [a] and relevant numbering scheme. Underlined compounds have been characterized by X-ray crystallography.

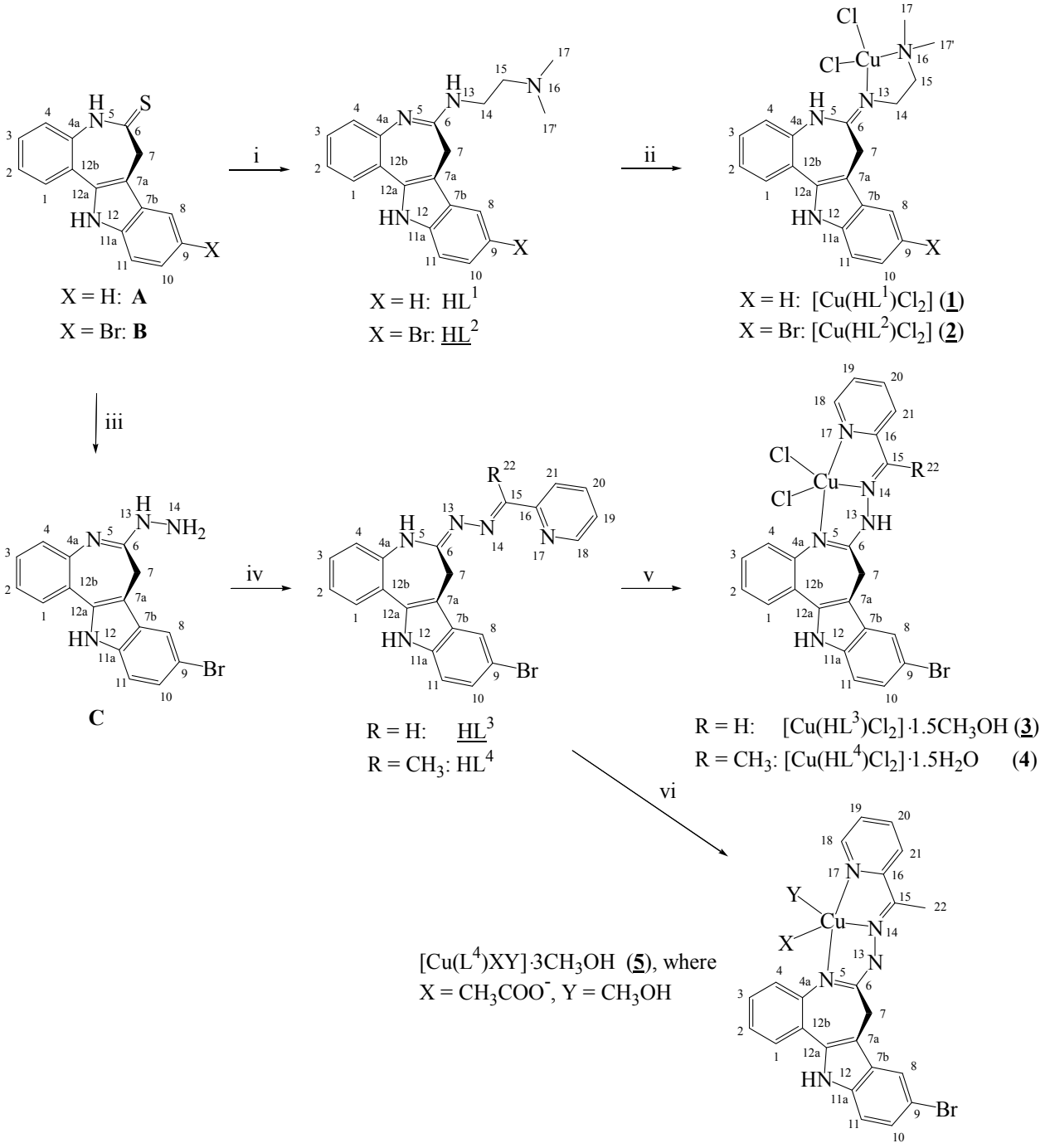

[a] Reagents and conditions: (i) N,N-dimethylethylenediamine, THF, Ar, reflux, 24 h (HL^1, 60%) or 45 h (HL^2, 68%); (ii) $CuCl_2\cdot 2H_2O$, CH_3OH, reflux, 30 min [68% (**1**), 69% (**2**)]; (iii) $N_2H_4\cdot H_2O$, C_2H_5OH, reflux, 1.5 h (85%); (iv) 2-pyridinecarbaldehyde, CH_3OH, reflux, 45 min (HL^3 68%) or 2-acetylpyridine, CH_3OH, reflux, 3.5 h (HL^4 73%); (v) $CuCl_2\cdot 2H_2O$, CH_3OH, reflux, 30 min [95% (**3**), 91% (**4**)]; (vi) $Cu(CH_3COO)_2\cdot H_2O$, CH_3OH, reflux, 30 min (83%) (**5**).

Experimental

Starting Materials. 7,12-dihydroindolo[3,2-*d*][1]benzazepin-6(5*H*)-thione (**A**),[58] 9-bromo-7,12-dihydroindolo[3,2-*d*][1]benzazepin-6(5*H*)-thione (**B**),[17] 9-Bromo-7,12-dihydroindolo[3,2-*d*][1]benzazepin-6-ylhydrazine (**C**),[20] 6-N-(2-N′,N′-dimethylaminoethylamino)-7,12-dihydroindolo-[3,2-*d*][1]benzazepine (HL^1) [59] and N-(9-Bromo-7,12-dihydroindolo[3,2-*d*][1]benzazepin-6(5*H*)-yliden-N'-(1-pyridin-2-yl-ethylidene)azine (HL^4) [60] were prepared according to published protocols. Tetrahydrofuran and ethanol were dried using standard procedures. Methanol (HPLC grade) was purchased from Fisher Scientific. Hydrazine hydrate, N,N-dimethylethylenediamine, 2-pyridinecarbaldehyde, 2-acetylpyridine and copper(II) chloride were purchased from Sigma-Aldrich and used without further purification.

9-Bromo-6-N-(2-N′,N′-dimethylaminoethylamino)-7,12-dihydroindolo-[3,2-*d*][1]benzazepine (HL^2). To 9-bromo-7,12-dihydroindolo[3,2-*d*][1]benzazepin-6(5H)-thione (**B**) (1.01 g, 3.0 mmol) in dry THF (60 ml), N,N-dimethylethylendiamine (0.38 ml, 3.5 mmol) was added and the reaction mixture was heated to reflux under argon for 45 h. Afterwards the solvent was evaporated and the solid residue extracted with diethyl ether (120 ml). The filtered extract was evaporated to ca. 50% of the initial volume and allowed to stand at –20 °C overnight. The colorless crystals formed were removed by filtration, washed with diethyl ether and dried *in vacuo*. Yield: 0.78 g, 68%. Anal. Calcd for $C_{20}H_{21}N_4Br$ (M_r = 397.31 g/mol) (%): C, 60.46; H, 5.33; N, 14.10. Found: C, 60.52; H, 5.63; N, 13.78. ^{1}H NMR (DMSO-d_6, δ): 11.61 (s, 1H, N12), 7.84 (s, 1H, C8), 7.68 (d, 1H, $^3J(H_{C2})$ = 7.5 Hz, C1), 7.36 (d, 1H, $^3J(H_{C10})$ = 8.5 Hz, C11), 7.25 (dd, 1H, $^3J(H_{C2})$ = 8.5 Hz, $^3J(H_{C4})$ = 8.0 Hz, C3), 7.23 (d, 1H, $^3J(H_{C11})$ = 8.5 Hz, C10), 7.14 (t, 1H, $^3J(H_{C14})$ = 5.0 Hz, N13), 7.13 (d, 1H, $^3J(H_{C3})$ = 8.0 Hz, C4), 7.03 (dd, 1H, $^3J(H_{C1})$ = 7.5 Hz, $^3J(H_{C3})$ = 8.5 Hz, C2), 3.32 (s, 2H, C7), 3.28 (dt, 2H, $^3J(H_{N13})$ = 5.0 Hz, $^3J(H_{C15})$ = 6.5 Hz, C14), 2.15 (s, 6H, C17+C18); $^{13}C\{^1H\}$ NMR

(DMSO-d_6, δ): 155.52 (C6), 147.25 (C4a), 136.78 (C11a), 136.24 (C12a), 129.09 (C7b), 128.36 (C4), 128.23 (C3), 127.42 (C1), 124.49 (C10), 122.59 (C12b), 121.07 (C2), 121.00 (C8), 113.96 (C11), 112.01 (C9), 109.31 (C7a), 58.61 (C15), 46.12 (C17+C18), 39.90 (C14), 28.66 (C7). UV–vis (DMSO), λ_{max} (ε, M^{-1} cm^{-1}): 263 (45000), 280 (44000), 319 (41000). Single crystals of $HL^2 \cdot C_2H_5OH$ suitable for X-ray diffraction study were obtained by slow evaporation of ethanolic solution of HL^2 at room temperature.

N-(9-Bromo-7,12-dihydroindolo[3,2-*d*][1]benzazepin-6(5*H*)-yliden-N'-(1-pyridin-2-yl-methylidene)azine (HL^3). To a refluxing suspension of **C** (0.25 g, 0.73 mmol) in methanol (62 ml), 2-pyridinecarbaldehyde (0.08 g, 0.74 mmol) was added. As soon as all starting material had dissolved, the reaction mixture was filtered hot, cooled to room temperature and allowed to stand at –20 °C overnight. The yellow precipitate formed was removed by filtration, washed with diethyl ether and dried *in vacuo*. Yield: 0.21 g, 68%. Anal. Calcd for $C_{22}H_{16}N_5Br \cdot H_2O$ (M_r = 448.32 g/mol) (%): C, 58.94; H, 4.05; N, 15.62. Found: C, 59.23; H, 4.17; N, 15.62. ^{1}H NMR (DMSO-d_6, δ): 11.82 (s, 1H, N12), 9.41 (s, 1H, N5), 8.59(d, 1H, $^3J(H_{C19})$ = 4.7 Hz, C18), 8.40 (d, 1H, $^3J(H_{C20})$ = 8.2 Hz, C21), 8.34 (s, 1H, C15), 7.92 (s, 1H, C8), 7.84 (dd, 1H, $^3J(H_{C19})$ = 7.3 Hz, $^3J(H_{C21})$ = 7.9 Hz, C20), 7.74 (d, 1H, $^3J(H_{C2})$ = 7.9 Hz, C1), 7.54 (d, 1H, $^3J(H_{C3})$ = 7.6 Hz, C4), 7.41 (dd, 1H, $^3J(H_{C2})$ = 7.5-8.5 Hz, $^3J(H_{C4})$ = 8.0 Hz, C3), 7.39 (d, 1H, $^3J(H_{C10})$ = 7.7 Hz, C11), 7.38 (dd, 1H, $^3J(H_{C18})$ = 4.0 Hz, $^3J(H_{C20})$ = 7.5 Hz, C19) 7.28 (dd, 1H, $^3J(H_{C1})$ = 7.9 Hz, $^3J(H_{C3})$ = 7.5-8.5 Hz, C2), 7.27 (d, 1H, $^3J(H_{C11})$ = 8.5 Hz, C10), 3.7 (s, 2H, C7); $^{13}C\{^1H\}$ NMR (DMSO-d_6, δ): 160.31 (C6), 154.77 (C15), 154.25 (C16), 149.77 (C18), 136.88 (C4a), 136.85 (C20), 136.35 (C11a), 134.74 (C12a), 128.73 (C3), 128.63 (C7b), 127.68 (C1), 124.98 (C10), 124.81 (C19), 124.03 (C2), 124.00 (C4), 122.95 (C12b), 121.85 (C21), 120.87 (C8), 113.90 (C11), 112.22 (C9), 109.48 (C7a), 27.66 (C7). UV–vis (DMSO), λ_{max} (ε, M^{-1} cm^{-1}): 268 (15300), 317 (25400), 339 (22200), 462

(760). X-ray diffraction quality single crystals of $HL^3 \cdot 2CH_3OH$ were picked up directly from the reaction vessel.

6-N-(2-N',N'-dimethylaminoethylenamino)-7,12-dihydroindolo[3,2-*d*][1]-benzazepino-dichlorido-copper(II) [Cu(HL^1)Cl$_2$] (**1**). To a solution of HL^1 (0.26 g, 0.81 mmol) in methanol (23.5 ml) under reflux, $CuCl_2 \cdot 2H_2O$ (0.14 g, 0.84 mmol) in methanol (1.5 ml) was added. The greenish-brown solution formed was refluxed for 5 min, filtered hot and allowed to cool to room temperature. The next day the crystals formed were removed by filtration, washed with methanol and dried *in vacuo*. Yield: 0.25 g, 69%. Anal. Calcd for $C_{20}H_{22}N_4Cl_2Cu$ (M_r = 452.88 g/mol) (%): C, 53.04; H, 4.90; N, 12.37. Found: C, 53.05; H, 4.90; N, 12.28. ESI-MS in methanol (positive): 274 $[HL^1-N(CH_3)_2]^+$, 319 $[H_2L^1]^+$, 380 $[Cu(L^1)]^+$, 416 $[Cu(HL^1)Cl]^+$, 440 unidentified, 454 $[Cu(L^1)ClK]^+$, 470 $[Cu(HL^1)Cl(CH_3O)Na]^+$. IR spectrum in KBr, selected bands, cm^{-1}: 3318, 3213, 3048, 2093, 1628, 1407, 768, 741. UV−vis (DMSO), λ_{max} (ε, M^{-1} cm^{-1}): 263 (26700), 323 (17300). Single crystals of **1** suitable for X-ray diffraction study were picked up directly from the reaction vessel.

9-Bromo-6-N-(2-N',N'-dimethylaminoethylenamino)-7,12-dihydroindolo[3,2-*d*][1]-benzazepino-dichlorido-copper(II) [Cu(HL^2)Cl$_2$] (2). To a refluxing solution of HL^2 (0.20 g, 0.51 mmol) in methanol (10 ml), a solution of $CuCl_2 \cdot 2H_2O$ (0.09 g, 0.52 mmol) in methanol (1 ml) was added. The dark-green solution formed was refluxed for 5 min, filtered hot and allowed to cool to room temperature. The next day the crystals formed were removed by filtration, washed with methanol and dried *in vacuo*. Yield: 0.21 g, 78%. Anal. Calcd for $C_{20}H_{21}N_4BrCl_2Cu$ (M_r = 531.76 g/mol) (%): C, 45.17; H, 3,98; N, 10.54. Found: C, 44.82; H, 4.04; N, 10.21. ESI-MS in methanol (positive): 352 $[HL^2-N(CH_3)_2]^+$, 397 $[H_2L^2]^+$, 458 $[Cu(L^2)]^+$, 494 $[Cu(HL^2)Cl]^+$, 518 unidentified, 532 $[Cu(L^2)ClK]^+$, 548 $[Cu(HL^2)Cl(CH_3O)Na]^+$. IR spectrum in KBr, selected bands, cm^{-1}: 3272, 1627, 1398, 807,

761, 748, 626. UV-vis (DMSO), λ_{max} (ε, M^{-1} cm^{-1}): 274 (31000), 317 (21000). Single crystals of **2** suitable for X-ray diffraction study were picked up directly from the reaction vessel.

N-(9-Bromo-7,12-dihydroindolo-[3,2-*d*][1]benzazepin-6-yliden)-N'-(1-pyridin-2-yl-methylidene)-azin-5-ide-dichlorido-copper(II) [Cu(L^3)Cl_2]·1.5CH_3OH (**3**). To a solution of HL^3 (0.04 g, 0.10 mmol) in methanol (7 ml) under reflux, $CuCl_2·2H_2O$ (0.019 g, 0.11 mmol) in methanol (1 ml) was added. The yellowish-brown solution formed was filtered hot and allowed to cool to room temperature. The next day the crystals formed were removed by filtration, washed with methanol and dried in air. Yield: 0.06 g, 64%. Anal. Calcd for $C_{22}H_{16}N_5BrCl_2Cu·1.5CH_3OH$ (M_r = 612.81 g/mol) (%): C, 46.06; H, 3.62; N, 11.43. Found: C, 46.06; H, 3.33; N, 11.38. ESI-MS in methanol (positive): 430 $[H_2L^3]^+$, 491 $[Cu(L^3)]^+$, 549 $[Cu(L^3)ClNa]^+$, 573 $[(L^3)Cu(CH_3OH)_2(H_2O)]^+$. IR spectrum in KBr, selected bands, cm^{-1}: 3015, 1618, 1546, 1400, 1303, 1021, 758, 738. UV-vis (DMSO), λ_{max} (ε, M^{-1} cm^{-1}): 311 (20300), 338 (16000), 463 (9700). Single crystals of the composition **3**·1.5CH_3OH suitable for X-ray diffraction study were picked up directly from the reaction vessel.

N-(9-Bromo-7,12-dihydroindolo-[3,2-*d*][1]benzazepin-6-yliden)-N'-(1-pyridin-2-yl-ethylidene)-azin-5-ide-dichlorido-copper(II) [Cu(HL^4)Cl_2]·1.5H_2O (**4**). To a suspension of HL^4 (0.11 g, 0.25 mmol) in refluxing methanol (19 ml) a solution of $CuCl_2·2H_2O$ (0.045 g, 0.26 mmol) in methanol (1 ml) was added. The reaction mixture was refluxed for 10 min, filtered hot and allowed to cool to room temperature. The next day the product formed was removed by filtration, washed with methanol and dried *in vacuo*. Yield: 0.13 g, 91%. Anal. Calcd for $C_{23}H_{18}N_5BrCl_2Cu·1.5H_2O$ (M_r = 605.80 g/mol) (%): C, 45.60; H, 3.49; N, 11.56. Found: C, 45.52; H, 3.30; N, 11.19. ESI-MS in methanol (positive): 505 $[Cu(L^4)]^+$, 587 $[(HL^4)Cu(CH_3O)CH_3OH(H_2O)]^+$. IR spectrum in KBr, selected bands, cm^{-1}: 3343, 3095, 3065, 1594, 1520, 1466, 1183, 770. UV–vis (DMSO), λ_{max} (ε, M^{-1} cm^{-1}): 310 (23000), 314

(20000), 454 (12800). Single crystals of the composition **4**·1.5H_2O suitable for X-ray diffraction study were picked up directly from the reaction vessel.

N-(9-Bromo-7,12-dihydroindolo-[3,2-*d*][1]benzazepin-6-yliden)-N'-(1-pyridin-2-yl-ethylidene)-azin-5-ide-acetato-methanolo-copper(II)

[Cu(L^4)(CH_3COO)(CH_3OH)]·3CH_3OH (**5**). To a suspension of HL^4 (0.445 g, 1.0 mmol) in refluxing methanol (9 ml) a solution of $Cu(CH_3COO)_2·H_2O$ (0.100 g, 0.5 mmol) in methanol (7 ml) was added. The dark-brown hot solution was filtered and saturated slowly with diethyl ether. After 3 days the crystals formed were removed by filtration, washed with methanol and dried in air. Yield: 0.30 g, 84%. Anal. Calcd for $C_{25}H_{20}N_5BrO_2Cu$ (M_r = 565.91 g/mol) (%): C, 53.06; H, 3.56; N, 12.38. Found: C, 52.83; H, 3.91; N, 12.76. ESI-MS in methanol (positive): 444 $[H_2L^4]^+$, 505 $[Cu(L^4)]^+$, 527 $[(L^4\text{-}H)CuNa]^+$, 593 $[HL^4CuK(CH_3O)H_2O]^+$. IR spectrum in KBr, selected bands, cm-1: 1634, 1491, 1461, 1387, 1152, 898, 762. UV–vis (methanol), λ_{max} (ε, M^{-1} cm^{-1}): 233 (52600), 261 (29600), 316 (30200), 436 (8500). Single crystals of the composition **5**·3CH_3OH suitable for X-ray diffraction study were picked up directly from the reaction vessel.

Physical Measurements. ^1H and ^{13}C NMR, NOE difference and two-dimensional ^1H-^1H COSY, ^1H-^1H TOCSY, ^1H-^{13}C HSQC and ^1H-^{13}C HMBC NMR spectra were recorded on a Bruker Avance III spectrometer (Ultrashield Magnet) in DMSO-d_6 at 25 °C using standard pulse programs at 500.10 (^1H) and 125.76 (^{13}C) MHz and a Bruker Avance DPX^{TM} 400 spectrometer (HL^2) at 400.13 (^1H) and (100.63 (^{13}C) MHz. ^1H and ^{13}C shifts are quoted relative to the residual solvent signals. Elemental analyses were carried out at the Microanalytical Service of the Institute of Physical Chemistry of the University of Vienna. Electrospray ionization mass spectrometry was carried out using a Bruker Esquire 3000 instrument (Bruker Daltonic, Bremen, Germany) on samples dissolved in methanol. Infrared spectra were obtained as KBr pellets on a Bruker Vertex 70 FT-IR spectrometer. UV–vis

spectra were recorded on a Perkin Elmer Lambda 650 spectrophotometer, using samples dissolved in DMSO (HL^1–HL^4 and **1–4**) and methanol (**5**). The aqueous solution behavior of HL^1–HL^2 and **1–4** with respect to hydrolysis was studied at 25 °C over 24 h by UV–vis spectroscopy in a 1.25% (v/v) DMSO-water mixture for HL^1, HL^2, **1** and **2**, and a 10% (v/v) DMSO-water mixture for **3** and **4**. Magnetic susceptibility measurements were conducted in solution on a Bruker Avance III spectrometer (Ultrashield Magnet) in DMSO-d_6 at 298 K using the Evans method. The μ_{eff} calculated for a 0.018 M $Cu(acac)_2$ solution in DMSO-d_6 was 1.75 μ_B.

Crystallographic Structure Determination. X-ray diffraction measurements were performed with Nonius Kappa CCP (HL^2) and Bruker X8 APEX II CCD diffractometers at 100 or 120 K (HL^2). Single crystals were positioned at 35, 35, 35, 30, 30 and 40 mm from the detector, and 525, 2619, 1643, 2017, 1374 and 3188 frames were measured, each for 50, 20, 60, 60, 60 and 20 s over 1.5, 1, 1, 1, 1, 1° scan width for HL^2, HL^3, **1–3** and **5**, respectively. The data were processed using the Denzo-SMN[61] or SAINT software package.[62] Crystal data, data collection parameters, and structure refinement details for HL^2, HL^3, **1–3** and **5** are given in Table 1. The structures were solved by direct methods and refined by full-matrix least-squares techniques. Non-hydrogen atoms were refined with anisotropic displacement parameters. H atoms were placed at calculated positions and refined as riding atoms in the subsequent least-squares model refinements. The isotropic thermal parameters were estimated to be 1.2 times the values of the equivalent isotropic thermal parameters of the non-hydrogen atoms to which hydrogen atoms were bonded. SHELXS-97[63] was used for structure solution and SHELXL-97[64] for refinement, molecular diagrams were produced with ORTEP,[65] and appropriate scattering factors were used.[66]

Cell lines and culture conditions. CH1 (ovarian carcinoma, human) cells were generously provided by Lloyd R. Kelland (CRC Centre for Cancer Therapeutics, Institute of Cancer Research, Sutton, U.K.). SW480 (colon carcinoma, human) and A549 (non-small cell lung cancer, human) cells were kindly provided by Brigitte Marian (Institute of Cancer Research, Department of Medicine I, Medical University of Vienna, Austria). Cells were grown without antibiotics in 75 cm^2 culture flasks (Iwaki/Asahi Technoglass) as adherent monolayer cultures in Minimal Essential Medium (MEM) supplemented with 10% heat-inactivated fetal bovine serum, 1 mM sodium pyruvate and 2 mM L-glutamine (all purchased from Sigma-Aldrich). Human A2780 and A2780cisR cells were obtained from the European Centre of Cell Cultures (ECACC, Porton down, Salisbury, UK) and cell culture reagents were obtained from Gibco-BRL (Basel, Switzerland). These cells were grown in RPMI 1640 medium containing 10% heat-inactivated fetal calf serum (FCS) and antibiotics. All cultures were maintained at 37 °C in a humidified atmosphere containing 5% CO_2 and 95% air.

Cytotoxicity determination. Cytotoxicity was determined by the colorimetric MTT assay (MTT = 3-(4,5-dimethyl-2-thiazolyl)-2,5-diphenyl-2H-tetrazolium bromide, Sigma-Aldrich). For this purpose, cells were harvested from culture flasks by trypsinization and seeded in 100 µL aliquots in the appropriate medium into 96-well microculture plates. The following cell densities were chosen to ensure exponential growth of untreated controls throughout the experiment: 1.5×10^3 (CH1), 2.5 x 10^3 (SW480) and 4.0×10^3 (A549) viable cells per well. For 24 h, cells were allowed to settle and resume exponential growth, followed by the addition of dilutions of the test compounds in aliquots of 100 µL/well in the same medium. For this purpose, the compounds (with the exception of copper chloride) were pre-dissolved in DMSO and then diluted with medium to a maximum DMSO content of 0.5% v/v. After continuous exposure for 96 or 72 h, medium was replaced by 100 µL/well RPMI 1640 medium (supplemented with 10% heat-inactivated fetal bovine serum and 4 mM L-glutamine)

plus 20 μL/well solution of MTT in phosphate-buffered saline (5 mg/mL) (all purchased from Sigma-Aldrich). After incubation for 4 h, medium/MTT mixtures were removed, and the formazan product formed by viable cells was dissolved in DMSO (150 μL/well). Optical densities at 550 nm were measured with a microplate reader (Tecan Spectra Classic), using a reference wavelength of 690 nm to correct for unspecific absorption. The quantity of viable cells was expressed as a percentage of the untreated controls, and 50% inhibitory concentrations (IC_{50}) were calculated from concentration-effect curves by interpolation. The evaluation is based on at least three independent experiments, each comprising three replicates per concentration level.

Results and discussion

The bidentate ligands HL^1 and HL^2 were prepared in good yield by reacting the thiones **A** and **B** (see Scheme 1) with N,N-dimethylethylenediamine in dry THF under reflux for 24 and 45 h, respectively. The Paullone-hydrazine **C** was obtained in 85% yield by condensation of hydrazine hydrate with thione **B** in dry ethanol at reflux (Scheme 1).[20] Further reaction of **C** with 2-pyridinecarbaldehyde or 2-acetylpyridine, respectively, affords the tridentate ligands HL^3 and HL^4.[60] ^1H and ^{13}C NMR spectra of HL^3 and HL^4 in DMSO-d_6 revealed that both ligands adopt a configuration with an exocyclic $C^6{=}N^{13}$ bond (confirmed by the chemical shifts of C^6 and presence of a proton at N^5), in contrast to HL^1 and HL^2 with an endocyclic $C^6{=}N^5$ bond (see Experimental).[59]

Complexes **1**−**4** were obtained in good to excellent yield (68−95%), as shown in Scheme 1, by reacting the corresponding ligand with $CuCl_2{\cdot}2H_2O$ in refluxing methanol. Complex **5** was obtained in 84% yield from reaction of HL^4 with $Cu(CH_3COO)_2{\cdot}H_2O$ in methanol under reflux. Magnetic susceptibility measurements were carried out in DMSO at 298 K for

complexes **2** and **4** using the Evans method.[67,68] The calculated effective magnetic moments of 1.75 and 1.74 μ_B, respectively, are in accord with the d^9 electronic configuration of copper(II) with S = ½.

The formation of the complexes was confirmed by electrospray ionization mass spectra (ESI-MS, positive ion mode) in methanol, in which peaks that may be assigned to the ions $[Cu(L^{1-4})]^+$ with *m/z* values of 380 (**1**), 458 (**2**), 491 (**3**) and 505 (**4** and **5**) were observed. The formation of the $[H_2L^{1-4}]^+$ ion was observed for all complexes, with the exception of **4**. The presence of intense peaks assigned to $[H_2L^{1-4}]^+$ ions for **1** and **2** indicate their lower stability compared to complexes **3** and **4** towards dissociation. In the spectra of **4** the peak attributed to the ion $[CuL^4]^+$ has the highest relative intensity.

Crystal Structures. The molecular structure of HL^2 established by single crystal X-ray diffraction is shown in Figure 1 and selected bond lengths and bond angles are given in the caption.

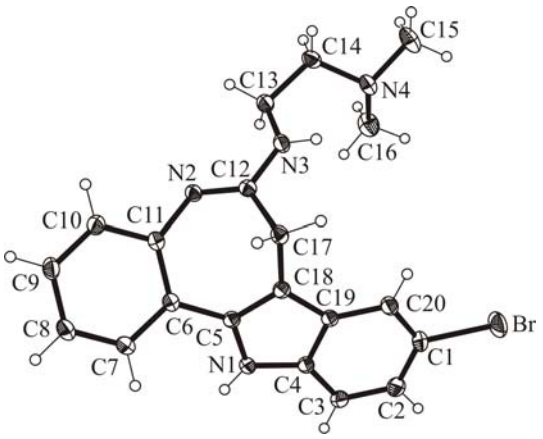

Figure 1. ORTEP plot of HL^2 with thermal ellipsoids drawn at the 50% probability level. Selected bond lengths (Å) and bond angles (deg): C11–N2 1.4141(16), C12–N2 1.3029(16), C12–N3 1.3460(16), C12–C17 1.5132(17), C17–C18 1.4954(17), C5–C18 1.3750(17), C5–C6 1.4592(17), C6–C11 1.4221(18) Å; $\Theta_{N1-C5-C6-C7}$ 36.84(18), $\Theta_{N3-C13-C14-N4}$ 48.20(15)°.

Complexes **1** and **2** (Fig. 2) crystallized in the monoclinic space group $P2_1/n$ and triclinic centrosymmetric space group $P\bar{1}$, respectively.

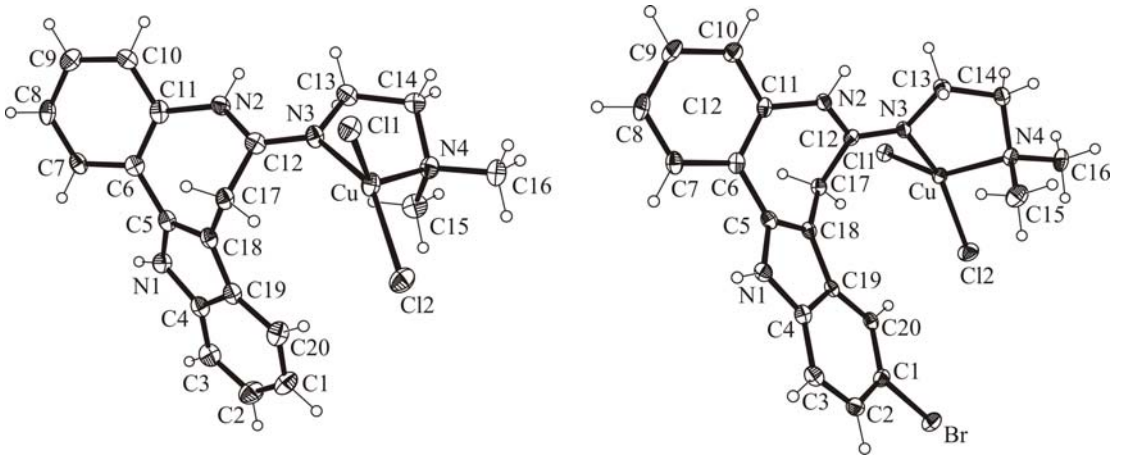

Figure 2. ORTEP plots for $[Cu(HL^1)Cl_2]$ (**1**) (left) and $[Cu(HL^2)Cl_2]$ (**2**) (right) with thermal ellipsoids drawn at the 50% probability level. Selected bond lengths (Å) and bond angles (deg) for **1**: Cu–Cl1 2.2715(9), Cu–Cl2 2.1965(10), Cu–N3 1.948(3), Cu–N4 2.021(3), C12–N2 1.347(4), C12–N3 1.301(4) Å; Cl1–Cu–N3 96.70(9), Cl1–Cu–N4 132.32(9), Cl2–Cu–N3 148.97(9), Cl2–Cu–N4 103.92(9), N3–Cu–N4 82.62(11) °; $\Theta_{N1–C5–C6–C7}$ 33.08(5), $\Theta_{N3–C13–C14–N4}$ 33.8(4); and for **2**: Cu–Cl1 2.2736(7), Cu–Cl2 2.2085(7), Cu–N3 1.975(2), Cu–N4 2.034(2), C12–N2 1.359(3), C12–N3 1.302(3) Å; Cl1–Cu–N3 96.96(6), Cl1–Cu–N4 147.45(6), Cl2–Cu–N3 151.99(6), Cl2–Cu–N4 96.72(6), N3–Cu–N4 81.77(9) °; $\Theta_{N1–C5–C6–C7}$ −35.3(4), $\Theta_{N3–C13–C14–N4}$ −32.4(3)°.

The copper(II) center in **1** and **2** is four-coordinate, and as expected, the ligands HL^1 and HL^2 are bound to the metal via two nitrogen atoms N3 and N4 of the ethylendiamine moiety. The remaining two binding sites are occupied by two chlorido ligands. The Cu–N and Cu–Cl distances are typical of those of other ethylenediamine derivatives of copper(II) chloride (e.g. $[Cu(ethylenediamine)Cl_2]$[69] Cu–N 2.010(5) and 2.017(5) Å, Cu–Cl 2.286(2) and 2.301(2) Å;

[Cu(*trans-N, N, N´,N´*-tetramethylcyclohexane-1,2-diamine)Cl_2[70] Cu–N 2.052(7), Cu–Cl 2.247(2) Å; [Cu(*N*-4-hydroxybenzylmethyl-*N,N´,N´*-trimethylethylenediamine)Cl_2][71] Cu–N 2.086(3) and 2.045(3) Å, Cu–Cl 2.263(1) and 2.269(1) Å. The coordination geometry can be described as a distorted tetrahedron. The distortion from the square-planar geometry in **1** and **2** may be estimated by the dihedral angle between the planes CuN3N4 and CuCl1Cl2, which deviates tremendously from 0° (55.8 and 41.7° for **1** and **2**, respectively).

The conformation of the coordinated ligand HL^2 differs to that adopted by the metal-free ligand (Fig. 1). This is evident when comparing the torsion angle $\Theta_{N1–C5–C6–C7}$ in metal-free HL^2 at 36.84 and in coordinated HL^2 in **2** at −35.3(4)°, which are of similar magnitude, but opposite sign. The ligand backbone mainly consists of sp^2-hybridized carbon and nitrogen atoms. The only exception is the methylene group carbon atom in the seven-membered azepine ring, which is sp^3-hybridized. This atom disrupts the conjugation of the whole π-system, and as a result the ligand as a whole is nonplanar. Binding to copper(II) is accompanied by rotation around the C5–C6 bond (Fig. 1), enabling azepine ring inversion and rotation of the dimethylamine group around the C13–C14 bond by 80.6°. It is also noteworthy that the distribution of electron density over the fragment N2–C12–N3 in **2** with an exocyclic C=N bond is opposite to that in the metal-free ligand HL^2 with an endocyclic C=N bond. The combined effect of these structural modifications possibly destabilize (weaken) the binding of the ethylenediamine-part of the ligand to the metal thereby reducing the overall stability of the complex in solution, notably in water which is nucleophilic (see below).

The crystal structure of **2** consists of molecules that are involved in two intermolecular hydrogen bonding interactions, namely N1–H···$Cl1^i$ [N1–H 0.88, H···$Cl1^i$ 2.371, N1···$Cl1^i$ 3.234 Å, N1–H···$Cl1^i$ 166.97] and N2–H···Cl^{ii} [N2–H 0.88, H···$Cl1^{ii}$ 2.625, N2···$Cl1^{ii}$ 3.416 Å, N2–H···$Cl1^{ii}$ 150.06], see Fig. S1.

The solid state structures of HL^3, **3** and **5** are shown in Figures 3–5, respectively. Selected bond distances (Å) and bond angles (deg) are given in the legends to Figures. The tridentate ligand HL^3 crystallized in the monoclinic space group $P2_1/c$ with two molecules of methanol. Intermolecular H-bonding interactions of the type O–H···N are evident between lattice methanol molecules and HL^3, namely O2···H–N12 (O2···H 1.920, O6···N12 2.780, H–N12 0.88 Å, O6···H–N12 165.24°), O2–H···N13 (O2–H 0.84, O2–N13 2.734, N13···H 1.911 Å, O2–H···N13 166.00°), O1···H–N5 (O1···H 2.144, O1···N5 3.010, H–N12 0.88 Å, O1···H–N12 168.17°), O1–H···N14 (O1–H 0.84, O1···N14 3.026, H···N14 2.497 Å, O1–H···N14 121.81°), O1–H···N17 (O1–H 0.84, O1···N17 2.904, H···N17 2.101 Å, O1–H···N17 159.92°). The distribution of electron density over the fragment N5–C6–N13 [C6–N5 1.358(5), C6–N13 1.309(5) Å] indicates the presence of an exocyclic double bond at the amidrazone moiety, which is in accordance with ^1H and ^{13}C NMR data for HL^3.

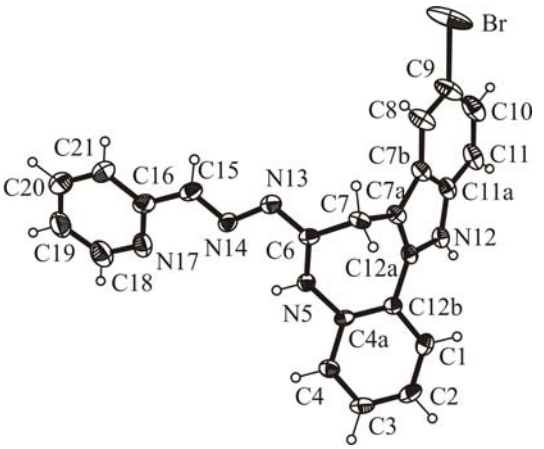

Figure 3. ORTEP plot of HL^3 with thermal ellipsoids drawn at the 50% probability level. Selected bond lengths (Å) and bond angles (deg): C4a–N5 1.410(5), C6–N5 1.358(5), C6–N13 1.309(5), N13–N14 1.399(5), N14–C15 1.274(6) Å; $\Theta_{N5-C6-N13-N14}$ −1.5(5), $\Theta_{C4a-N5-C6-C7}$ −2.6(7), $\Theta_{N12-C12a-C12b-C1}$ 34.0(6)°.

Complex **3** crystallized in the monoclinic space group $P2_1/c$ with 0.75 molecules of lattice water. As expected, HL^3 acts as a neutral tridentate ligand in **3**. Copper(II) is coordinated via the azepine ring nitrogen atom N5, the hydrazine group nitrogen atom N14, and the pyridine ring nitrogen atom N17.

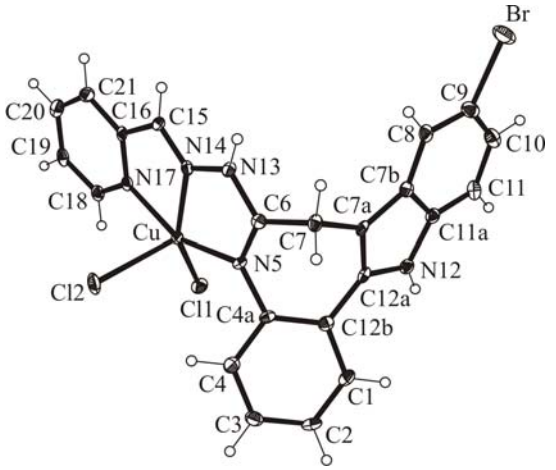

Figure 4. ORTEP plot of $[Cu(HL^3)Cl_2]$ (**3**) with thermal ellipsoids drawn at the 50% probability level. Selected bond lengths (Å) and bond angles (deg): Cu–N5 2.038(3), Cu–N14 1.982(3), Cu–N17 2.062(3), Cu–Cl1 2.2411(8), Cu–Cl2 2.4306(8), C6–N5 1.296(4), C6–N13 1.366(4), N13–N14 1.353(3); N5–Cu–N17 155.53(10), N14–Cu–Cl2 103.39(7), N14–Cu–Cl1 149.67(8), Cl1–Cu–Cl2 106.63(3), N5–Cu–Cl2 100.75(7), N5–Cu–Cl1 100.01(7), N14–Cu–N17 77.75(10), N17–Cu–Cl2 89.52(7), N17–Cu–Cl1 98.18(7).

Complex **5** crystallized in the triclinic centrosymmetric space group $P\bar{1}$ (**5**) with three molecules of methanol in the asymmetric unit, involved in strong intermolecular H-bonding interactions of the type O–H···O between lattice methanol molecules [O6···O5(x – 1, y, z) 2.772, O4···O5(–x + 2, –y + 2, –z + 1) 2.892 Å], between lattice methanol molecules and **5**, namely O6···H–N12 (O6···H 1.913, O6···N12 2.760, H–N12 0.88 Å, O6···H–N12 160.89°), O5–H···O2(x + 1, y, z) with O5–H 0.84, H···O2 1.844, O5···O2 2.651 Å, O5–H···O2 160.53°

and between molecules of **5** of the type O3–H···N13(–*x* + 1, –*y* + 1, –*z* + 1) with O3–H 0.833, H···N13 1.970, O3···N13 2.795 Å, O3–H···N13 170.16° (Figure S2). As expected, HL^4 acts as a neutral tridentate ligand in **4** and as a monodeprotonated ligand in **5**, coordinating to copper(II) via the azepine ring nitrogen atom N5, the hydrazine group nitrogen atom N14, and the pyridine ring nitrogen atom N17. The copper(II) center is five-coordinate, the remaining two binding sites being occupied by two chloride ligands in **3** or by two different ligands, an acetate ion (atom O1) and a methanol (atom O3), in **5**.

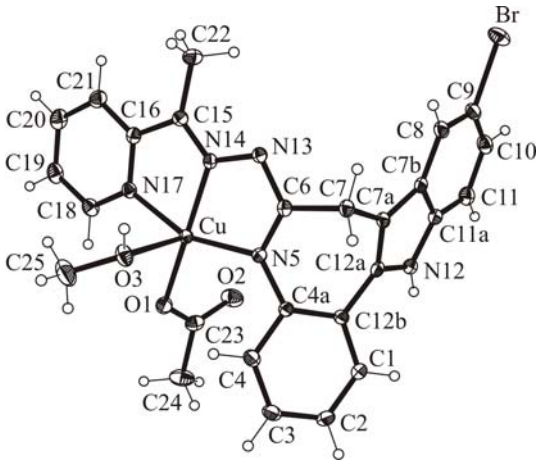

Figure 5. ORTEP plot of [Cu(L^4)(CH_3COO)(CH_3OH)] (**5**) with thermal ellipsoids drawn at the 50% probability level. Selected bond lengths (Å) and bond angles (deg): Cu–N5 1.9994(17), Cu–N14 1.9482(18), Cu–N17 2.0363(18), Cu–O1 1.9392(15), Cu–O3 2.2794(15), C6–N5 1.324(3), C6–N13 1.351(3), N13–N14 1.372(2); N5–Cu–N17 158.21(7), N14–Cu–O1 173.26(7), N14–Cu–O3 96.86(6), O1–Cu–O3 88.73(6), N5–Cu–O1 103.89(7), N5–Cu–O3 96.38(6), N14–Cu–N17 79.92(7), N17–Cu–O1 96.12(7), N17–Cu–O3 92.55(6).

The τ-descriptor for five-coordinate complexes expressed as the difference between the angles N5–Cu–N17 155.53(10) and N14–Cu–Cl1 149.67(8) divided by 60 gives a value of 0.10 for **3**, which is very close to the ideal one for a square pyramid (0).[72] Note that this value

in the five-coordinate gallium(III) complex $[Ga(L^4)Cl_2]$[60] is between that for a trigonal bipyramid (1) and that for a square pyramid (0) at 0.52. The angles between the mean plane of the indole moiety and the benzene ring annelated to the seven-membered azepine ring in **3** and **5** are 39.6 and 36.7°, respectively. These values are close to those in the metal-free ligands HL^3 (35.0°) and HL^4 (34.0°), and in $Ga(L^4)Cl_2$ (33.6°). In contrast the angle between the indole and the pyridine ring in **3** is 78.6° and in **5** is 83.6°, differing by ca. 54 and 49°, respectively, from that in the metal-free ligand HL^4 (132.56°) and by ca. 38 and 33°, respectively, to that in metal-free ligand HL^3 (116.39°). In contrast to HL^4, the bond lengths C6–N5 [1.324(3) Å] and C6–N13 [1.351(3) Å] differ from one another to a lesser extend and indicate a delocalized π-system, which also extends over the N13–N14 [1.372(2) Å] bond in **5**. The distribution of electron density over the fragment N5–C6–N13 [C6–N5 1.3621(16), C6–N13 1.3088(16) Å] indicates the presence of an exocyclic double bond at the amidrazone moiety. The lack of a proton at N13 is corroborated by the role of the amidrazone moiety as a proton acceptor from the coordinated methanol of the neighbouring molecule with formation of the hydrogen bond N13···H–O3 in **5**. The τ-descriptor for **5**, expressed as the difference between the angles N14–Cu–O1 173.26 and N5–Cu–N17 158.21 divided by 60, gives a value of 0.25, which is close to the ideal value for a square pyramid (0).[72]

Table 1. Crystal Data and Details of Data Collection for HL^2, HL^3, **1–3** and **5**

Compound	HL^2	HL^3	**1**	**2**	**3**	**5**
empirical formula	$C_{22}H_{27}BrN_4O$	$C_{24}H_{24}BrN_5O_2$	$C_{20}H_{22}Cl_2CuN_4$	$C_{20}H_{21}BrCl_2CuN_4$	$C_{22}H_{17.5}BrCl_2CuN_5O_{0.75}$	$C_{29}H_{36}BrCuN_5O_6$
fw	443.39	486.38	452.86	531.76	578.26	694.08
space group	$P2_1/c$	$P2_1/c$	$P2_1/n$	$P\bar{1}$	$P2_1/c$	$P\bar{1}$
a, Å	10.978(2)	12.3094(5)	15.1349(9)	10.1511(5)	12.7662(8)	9.2218(3)
b, Å	9.193(2)	11.1450(4)	7.6083(5)	10.8098(6)	13.5586(8)	12.6553(5)
c, Å	21.116(4)	17.0199(7)	17.3917(11)	11.7944(9)	13.1869(8)	13.7218(6)
α,deg				113.613(4)		107.719(3)
β, deg	94.93(3)	97.995(2)	101.579(4)	93.568(4)	105.691(4)	90.188(2)
γ,deg				115.547(3)		98.000(2)
V, Å^3	2123.2(7)	2312.24(16)	1508.81(10)	1025.78(11)	2197.5(2)	1508.81(10)
Z	4	4	4	2	4	2
λ, Å	0.71073	0.71073	0.71073	0.71073	0.71073	0.71073
ρ_{calcd}, g cm^{-3}	1.387	1.420	1.533	1.722	1.748	1.528
crystal size, mm	0.57 × 0.29 × 0.23	0.20 × 0.18 × 0.10	0.16 × 0.11 × 0.02	0.15 × 0.08 × 0.03	0.10 × 0.10 × 0.07	0.40 × 0.15 × 0.08
T, K	120	120	100	100	100	100
μ, cm^{-1}	19.56	18.08	13.98	32.87	30.80	20.98
R1[a]	0.0308	0.0650	0.0423	0.0337	0.0396	0.0355
wR2[b]	0.0792	0.1932	0.0984	0.0800	0.0927	0.1008
GOF[c]	1.021	1.060	1.005	1.019	1.007	1.013

[a] $R1 = \Sigma||F_o| - |F_c||/\Sigma|F_o|$, [b] $wR2 = \{\Sigma[w(F_o^2 - F_c^2)^2]/\Sigma[w(F_o^2)^2]\}^{1/2}$. [c] $GOF = \{\Sigma[w(F_o^2 - F_c^2)^2]/(n-p)\}^{1/2}$, where *n* is the number of reflections and *p* is the total number of parameters refined.

Stability studies. The kinetic stability of the complexes in aqueous solution with a DMSO content of 1.25% v/v (**1** and **2**) or 10% v/v (**3** and **4**) was studied by UV−vis spectroscopy over 24 h. For **1** and **2** the resulting spectra were compared with those of the ligands HL^1 and HL^2 (Figures S3 and S4). A weak charge-transfer band at 397 nm (Figures S5 and S6) with a molar extinction coefficient of ca. 570 $M^{-1}cm^{-1}$, resulting from coordination of ethylenediamine moiety to copper(II) ion, seems to be responsible for the yellow color of the methanol solutions of **1** and **2**. As the spectra of **1** and **2** are very similar to those of the corresponding ligands, no clear statement can be made whether **1** and **2** dissociate or hydrolyze during the measurements in aqueous DMSO solution. However, ESI mass spectra of **1** and **2** in a methanolic solution with 10% water measured 24 h after dissolution showed the presence of peaks with *m/z* values of 319 and 397, attributable to $[H_2L^1]^+$ and $[H_2L^2]^+$ correspondingly, indicating their dissociation or hydrolysis. In contrast, on coordination of ligands HL^3 and HL^4 to copper(II) via the pyridine nitrogen atom, the hydrazine nitrogen and the azepinone ring nitrogen atom alters significantly the conjugated π-systems of the yellow colored ligands HL^3 and HL^4, resulting in significantly different electronic absorption spectra. As a result, solutions of **3** and **4** show significant absorbances in the visible range, namely a broad charge-transfer band at 430 and 420 nm, respectively (Fig. S7). These bands are blue-shifted by 29 and 27 nm for **3** and **4**, respectively, when DMSO as solvent is replaced by water with a content of 10% DMSO (v/v). A small decrease in absorption (ca. 4%) for **3** and **4** was observed over the first 4 h, with no further changes over the next 20 h, indicating that the coordination sphere of copper(II) remained intact.

Biological studies. The cytotoxicity of **1**, HL^1, **2**, HL^2, **3** and **4** was assessed by means of a colorimetric microculture assay (MTT assay) in three human cancer cell lines (A549, SW480, CH1). Additionally, complexes **1**, **2** and **4** were tested in an isogenic pair of cell lines, one being sensitive to cisplatin (A2780) and the other having acquired cisplatin resistance

(A2780cisR). The compounds showed the strongest effects on cell viability on the more chemosensitive ovarian carcinoma cell line CH1, whereas the more chemoresistant non-small cell lung cancer cell line A549 is the least sensitive for this series of compounds. The IC_{50} values are listed in Table 2, and the concentration-effect curves in three cell lines are depicted in Figures 6 and 7, from which certain structure-activity relationships can be discerned (see below).

The Paullone derived ligands HL^1 and HL^2 show notable cytotoxicities with IC_{50} values in the 10^{-6} or 10^{-5} M range. Substitution by bromine at position 9 of the Paullone scaffold has a favorable effect on cytotoxicity, as reflected by the significantly lower IC_{50} values of the HL^2 ligand. Previously this substitution has been reported to increase CDK-inhibitory potency, but apparently without being reflected in an enhanced cytotoxicity.[14] Complexation of the Paullones HL^1 and HL^2 with copper(II) results in only a modest increase in cytotoxicity. Only in CH1 cells is a clear-cut advantage of complexation of the HL^1 ligand with a significant improvement in cytotoxicity observed. Nevertheless, activity is maintained in the complexes, and other advantages relevant for the *in vivo* applications arise from their higher solubility and/or altered pharmacokinetic behavior. Comparison of the complexes **1** and **2** shows that bromination of the ligand at C9 results in a higher cytotoxicity, depending on the cell line (with the exception of A2780), roughly paralleling the effects in the uncomplexed Paullone derivatives (Figure 6).

The cytotoxic potencies of HL^3 and HL^4 could not be determined because of insufficient solubility, and while the compounds mentioned above show IC_{50} values in micromolar concentrations, complexes **3** and **4** exhibit cytotoxicities mainly in the nanomolar range. Thus, the structural modifications of the chelating side chain result in 4.7–12 and 11–33 times higher cytotoxicity, respectively, compared to complex **2**. As the cytotoxicities of HL^3 and HL^4 could not be determined because of insufficient solubility, it cannot be assessed whether

the modification of the side chain itself or the consequences for binding to copper, i.e. a tridentate coordination involving N5 of the azepine ring, accounts for the increase in activity. Thus, it remains unclear whether the effects of complexes **3** and **4** are governed by those of the ligands HL^3 and HL^4 to the same extent as the effects of **2** are by those of HL^2 or whether coordination to copper adds a more substantial component to overall activity in these cases. However, it is not unreasonable to assume that HL^1, HL^2, **1** and **2** exhibit similar cytotoxicities as the copper ion is released from the bidentate ligand whereas in **3** and **4** stronger coordination leads to an enhancement in activity. It is worth noting that the IC_{50} values of $CuCl_2$ range between 43 and > 160 μM and are thus one order of magnitude higher than those of the least cytotoxic complex (Table 2). If copper ions were partially released from the complexes at any stage of exposure, they are unlikely to contribute appreciably to the overall effects.

At least for the copper(II) complexes, the methyl substitution in position 15 of the Paullone ligand is favorable in terms of biological activity, as indicated by the lower IC_{50} values of complex **4** compared to **3**, yielding the most cytotoxic compound within the series (Figure 7).

The acquired cisplatin resistance of the ovarian cancer cell line A2780cisR affects sensitivity to complexes **1**, **2** and **4** to only a moderate extent, as indicated by slightly higher IC_{50} values than in the parent A2780 cell line (Table 2). As resistance in A2780cisR cells does not exclusively pertain to DNA cross-linking agents and can only partially be attributed to increased DNA repair capacity,[73] DNA-damaging effects cannot be inferred unequivocally from these data, but should be considered in future mechanistic studies of the copper(II) complexes.

Table 2. Cytotoxicity of Paullone-based ligands, their copper(II) complexes and $CuCl_2$ in human cancer cell lines.

Compound	IC_{50} (μM)[a]				
	A549 [a]	SW480 [a]	CH1 [a]	A2780 [b]	A2780cisR [b]
HL[1]	44 ± 1	25 ± 1	21 ± 3	–	–
HL[2]	8.2 ± 1.0	4.5 ± 0.4	3.0 ± 0.4	–	–
1	39 ± 5	12 ± 2	3.2 ± 0.2	3.6 ± 0.4	10 ± 1
2	9.9 ± 1.3	4.0 ± 0.4	1.6 ± 0.04	4.0 ± 0.2	5.2 ± 0.5
3	1.2 ± 0.2	0.33 ± 0.06	0.34 ± 0.06	–	–
4	0.35 ± 0.04	0.12 ± 0.004	0.050 ± 0.003	0.19 ± 0.04	0.49 ± 0.05
$CuCl_2$	153 ± 8	> 160	43 ± 3	–	–

50% inhibitory concentrations (means ± standard deviations from at least three independent experiments), as obtained by the MTT assay (exposure for [a] 96 h, or [b] 72 h).

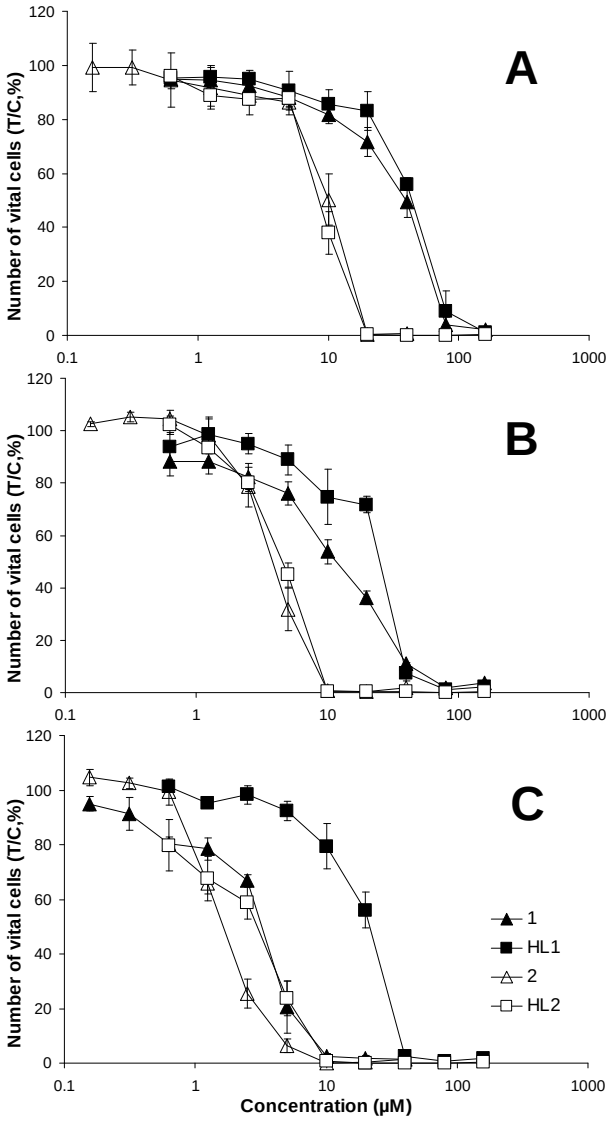

Figure 6. Concentration-effect curves of complexes **1** and **2** in comparison with the corresponding uncomplexed Paullone derivatives HL^1 and HL^2 in the human cancer cell lines A549 (A), SW480 (B) and CH1 (C), obtained by the MTT assay following continuous exposure for 96 h.

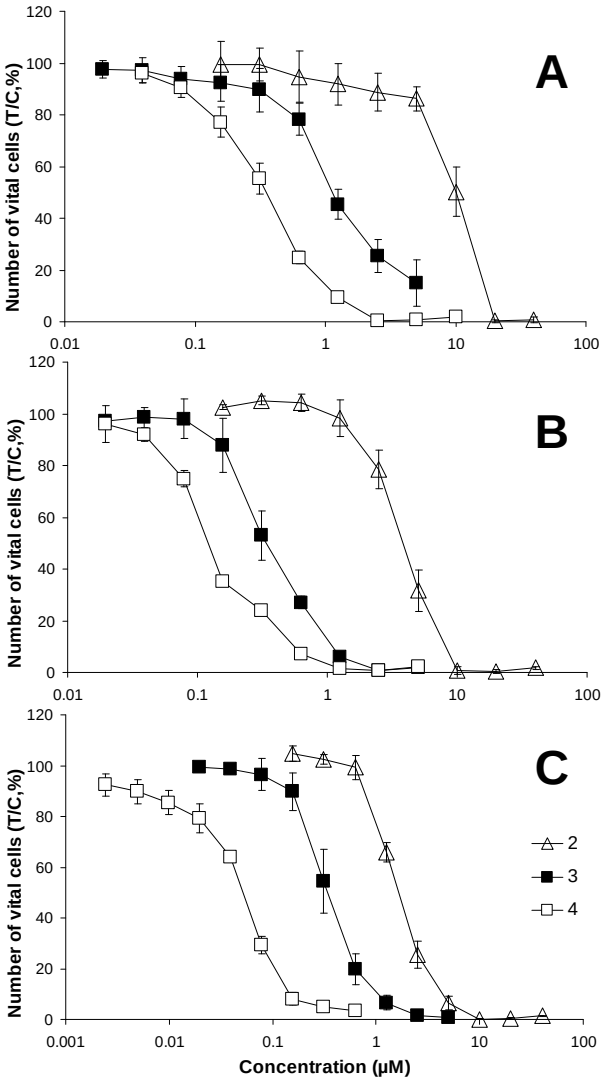

Figure 7. Concentration-effect curves of complexes **2**, **3** and **4** in the human cancer cell lines A549 (A), SW480 (B) and CH1 (C), obtained by the MTT assay following continuous exposure for 96 h.

Final remarks. Complexation of copper(II) salts with bidentate and tridentate Paullone-based ligands HL^{1-2} and HL^{3-4} modified at the lactone function resulted in four-coordinate (**1** and **2**) and five-coordinate (**3**−**5**) copper(II) complexes, which show markedly different, but remarkably high, antiproliferative activities in human cancer cell lines with IC_{50} values in the micromolar (**1**, **2**) or in the nanomolar (**3**, **4**) concentration range. The high cytotoxicity of the metal-free Paullones HL^{1-2} is at least preserved upon binding to copper(II) or even enhanced, as in the case of HL^1 and **1** in CH1 cells. It should be also stressed that the biological activity

of metal-free Paullones HL^{3-4} could not be assayed because of their very low solubility in biocompatible media. Coordination to copper(II) improved the solubility of the resulted species, enabling them to be used as anticancer agents. It is highly probable that for **3** and **4** the copper(II) center remains attached to the Paullone ligands until entry into the cells, although it remains to be established whether the metal ion is cleaved once inside the cell. Further experiments are in progress to delineate the mode of action of these compounds. The fact that **3** and **4** are highly cytotoxic, at nanomolar concentrations, could allow their application at very low doses which could offer a significant advantage over platinum-based chemotherapies.

Acknowledgment. We would like to thank Mr. Werner Ginzinger for his contribution to the synthesis of HL2, Mr. Alexander Roller for collection of X-ray diffraction data, as well as Mr. Anatolie Dobrov and Prof. Dr. Markus Galanski for recording ESI-MS and NMR spectra.

References

(1) Ang, W.H.; Dyson, P.J. *Eur. J. Inorg. Chem.* **2006**, *20*, 4003–4018.

(2) Heffeter, P.; Jungwirth, U.; Jakupec, M.; Hartinger, C.; Galanski, M.; Elbling, L.; Micksche, M.; Keppler, B.; Berger, W. *Drug Resist. Update* **2008**, *11*, 1–16.

(3) Frezza, M.; Hindo, S. S.; Tomco, D.; Allard, M. M.; Cui, Q. C.; Heeg, M. J.; Chen, D.; Dou, Q. P.; Verani, C. N. *Inorg. Chem.* **2009**, *48*, 5928–5937.

(4) Hindo, S. S.; Frezza, M.; Tomco, D., Heeg, M. J.; Hryhorczuk, L.; McGarvey, B. R.; Dou, Q. P.; Verani, C. N. *Eur. J. Med. Chem.* **2009**, *44*, 4353–4361.

(5) Galanski, M.; Arion, V. B.; Jakupec M. A.; Keppler, B. K. *Curr. Pharm. Design* **2003**, *9*, 2078–2089.

(6) Yu, Y.; Wong, J.; Lovejoy, D. B.; Kalinowski, D. S.; Richardson, D. R. *Clin. Cancer Res*. **2006**, *12*, 6876–6883.

(7) Bolos, C. A.; Chaviara, A. T.; Mourelatos, D.; Iakovidou, Z.; Mioglou, E.; Chrysogelou, E.; Papageorgiou, A. *Bioorg. Med. Chem*. **2009**, *17*, 3142–3151.

(8) Sathisha, M. P.; Shetti, U. L.; Revankar, V. K.; Pai, K. S. R. *Eur. J. Med. Chem.* **2008**, *43*, 2338–2346.

(9) Peters, J. Z.; Nykamp, J. A.; Passaperuma, K.; Carlson, J. C.; DeWitte-Orr, S. J.; Greenberg, B. N.; Bols, N. C. *Reprod. Toxicol.* **2007**, *23*, 513–520.

(10) Debreczeni, J.É.; Bullock, A.N.; Atilla, G.E.; Williams, D.S.; Bregman, H.; Knapp, S.; Meggers, E. *Angew. Chem. Int. Ed.* **2006**, *45*, 1580 –1585.

(11) Zhang, L.; Carroll, P.; Meggers, E. *Org. Lett.* **2004**, *6*, 521–523.

(12) Bregman, H.; Carroll, P.J.; Meggers, E. *J. Am. Chem. Soc.* **2006**, *128*, 877–884.

(13) Zagermann, J.; Kuchta, M.C.; Merz, K.; Metzler-Nolte, N. *J. Organomet. Chem.* **2009**, *694*, 862–867.

(14) Zaharevitz, D. W.; Gussio, R.; Leost, M.; Senderowicz, A. M.; Lahusen, T.; Kunick C.; Meijer, L.; Sausville, E. A. *Cancer Res.* **1999**, *59*, 2566–2569.

(15) Knockaert, M.; Wieking, K.; Schmitt, S.; Leost, M.; Grant, K. M.; Mottram, J. C.; Kunick, C.; Laurent, M. J. *Biol. Chem.* **2002**, *277*, 28, 25493–25501.

(16) Trapp, J.; Jochum, A.; Meier, R.; Saunders, L.; Marshall B.; Kunick, C.; Verdin E.; Goekjian P.; Sippl, W.; Jung, M. *J. Med. Chem.* **2006**, *49*, 7307–7316.

(17) Schultz, C.; Link, A.; Leost, M.; Zaharevitz, D. W.; Gussio R.; Sausville, E. A.; Meijer, L.; Kunick, C. *J. Med. Chem.* **1999**, *42*, 2909–2919.

(18) Schmid, W. F.; Zorbas-Seifried, S.; John, R. O.; Arion, V. B.; Jakupec, M. A.; Roller, A.; Galanski, M.; Chiorescu, I.; Zorbas, H.; Keppler, B. K. *Inorg. Chem.* **2007**, *46*, 3645–3656.

(19) Schmid, W. F.; John, R. O.; Muehlgassner, G.; Heffeter, P.; Jakupec, M. A.; Galanski, M.; Berger, W.; Arion, V. B.; Keppler, B. K. *J. Med. Chem.* **2007**, *50*, 6343–6355.

(20) Dobrov, A.; Arion, V. B.; Kandler, N.; Ginzinger, W.; Jakupec, M. A.; Rufinska, A.; Graf von Keyserlingk, N.; Galanski, M.; Kowol, C.; Keppler, B. K. *Inorg. Chem.* **2006**, *45*, 1945–1950.

(21) Schmid, W. F.; John, R. O.; Arion, V. B.; Jakupec, M. A.; Keppler, B. K. *Organometallics* **2007**, *26*, 6643–6652.

(22) Kraatz, H.-B.; Metzler-Nolte, N. *Concepts and Models in Bioinorganic Chemistry*; WILEY-VCH: Weinheim, Germany, 2006.

(23) Lippard, S. J.; Berg, J. M. *Principles of Bioinorganic Chemistry*; University Science Books: Mill Valley, CA, 1994.

(24) Harris, Z. H.; Gitlin, J. D. *Am. J. Clin. Nutr.* **1996**, *63*, 836S–841S.

(25) Fráusto da Silva, J. J. R.; Williams, R. J. P. *The Biological Chemistry of the Elements*, Clarendon: Oxford, 1991.

(26) Lonnerdal, B. *Am. J. Clin. Nutr.* **1996**, *63*, 821S–829S.

(27) Valko, M.; Morris, H.; Cronin, M. T. D. *Curr. Med. Chem.* **2005**, *12*, 1161–1208.

(28) Wang, T.; Guo, Z. *Curr. Med. Chem.* **2006**, *13*, 525–537.

(29) Tapiero, H.; Townsend, D. M.; Tew, K. D. *Copper Biomed. Pharmacother.* **2003**, *57*, 386–398.

(30) Hellman, N. E.; Gitlin, J. D. *Annu. Rev. Nutr.* **2002**, *22*, 439–458.

(31) Linder, M. C.; Wooten, L.; Cerveza, P.; Cotton, S.; Shulze, R.; Lomeli, N. *Am. J. Clin. Nutr.* **1998**, *67*, 965S–971S.

(32) Kim, B. E.; Nevitt, T.; Thiele, D. J. *Nat. Chem. Biol.* **2008**, *4*, 176–185.

(33) Arredondo, M.; Núñez, M.T. *Mol. Aspects Med.* **2005**, *26*, 313–327.

(34) Gupte, A.; Mumper, R. J. *Cancer Treat. Rev.* **2009**, *35*, 32–46.

(35) Brewer, G. *Drug Dicov. Today* **2005**, *10*, 1103–1109.

(36) Goodman, V. L.; Brewer, G. J.; Maerajver, S. D. *Endocr.-Relat. Cancer* **2004**, *11*, 255–263.

(37) Kuo, K. W.; Chen, S. F.; Wu, C. C.; Chen, D. R.; Lee, J. H. *Biol. Trace Elem. Res.* **2002**, *89*, 1–11.

(38) Scanni, A.; Licciardello, L.; Trovato, M.; Tomirotti, M.; Biraghi, M. *Tumori* **1977**, *63*, 175–180.

(39) Zuo, X. L.; Chen, J. M.; Zhou, X.; Li, X. Z.; Mei, G. Y. *Biol. Trace Elem. Res.* **2006**, *114*, 41–54.

(40) Chan, A.; Wong, F.; Arumanayagam, M. *Ann. Clin. Biochem.* **1993**, *30*, 545–549.

(41) Diez, M.; Arroyo, M.; Cerdan, F. J.; Munoz, M.; Martin, M. A.; Balibrea, J. L. *Oncology* **1989**, *46*, 230–234.

(42) Habib, F. K.; Dembinski, T. C.; Stitch, S. R. *Clin. Chim. Acta* **1980**, *104*, 329–335.

(43) Rajput, V. S.; Gupta, S. N.; Sur, B. K.; Pandey, R. P.; Singh, S. *Indian J. Surg.* **1979**, *5*, 515–519.

(44) Carpentieri, U.; Myers, J.; Thorpe, L.; Daeschner, C. W.; Haggard, M. E. *Cancer Res.* **1986**, *46*, 981–984.

(45) Jayadeep, A.; Pillai, K. R.; Kannan, S.; Nalinaumari, K. R.; Mathew, B.; Krishnan Nair, M.; Menon, V. P. *J. Exp. Clin. Cancer Res.* **1997**, *16*, 295–300.

(46) Lightman, A.; Brandes, J. M.; Binur, N.; Drugan, A.; Zinder, O. *Clin. Chem.* **1986**, *32*, 101–103.

(47) Huang, Y.-L.; Sheu, J. H.; Lin, T.-H. *Clin. Biochem.* **1999**, *32*, 131–136.

(48) Cohen, Y.; Epelbaum, R.; Haim, N.; Mcshan, D.; Zinder, O. *Cancer* **1984**, *53*, 296–300.

(49) Yucel, I.; Arpaci, F.; Ozet, A.; Doner, B.; Karayilanoglu, T.; Sayar, A.; Berk, O. *Biol. Trace Elem. Res.* **1994**, *40*, 31–37.

(50) Gupta, S. K.; Shukla, V. K.; Vaidya, M. P.; Roy, S. K.; Gupta, S. *J. Surg. Oncol.* **1991**, *46*, 178–181.

(51) Sharma, K.; Mittal, D. K.; Kesarwani, R. C.; Kamboj, V. P. *Ind. J. Med. Sci.* **1994**, *48*, 227–232.

(52) Folkman, J.; Klagsburn, M. *Science* **1987**, *235*, 442–447.

(53) Brewer, G. *Drug Discov. Today* **2005**, *10*, 1103–1109.

(54) Brem, S. *Cancer Control* **1999**, *6*, 436–458.

(55) Petering, D. H. *Met. Ions Biol. Syst.* **1980**, *11*, 197–229.

(56) (a) French, F. A.; Blanz Jr, E. J. *Cancer Res.* **1965**, *25*, 1454–1458; (b) **1966**, *26*, 1638–1640.

(57) Gielen, M.; Tieknik, E. R. T. *Metallotherapeutic Drugs and Metal-Based Diagnostic Agents: The Use of Metals in Medicine*; Wiley & Sons, Ltd., 2005.

(58) Kunick, C. *Liebigs Ann.Chem.* **1993**, 1141–1143.

(59) Filak, L. K., Mühlgassner, G., Jakupec, M. A.; Berger, W.; Arion, V. B.; Keppler, B. K. *J. Med. Chem.* submitted.

(60) Ginzinger, W.; Arion, V. B.; Giester, G.; Galanski, M.; Keppler, B. K. *Cent. Eur. J. Chem.* **2008**, *6*, 340–346.

(61) Otwinowski, Z.; Minor, W. *Macromolecular Crystallography, Part A*; Academic Press: New York, **1997**; Vol. 276, pp 307–326.

(62) SAINT-Plus (Version 7.06a) and APEX2. Bruker-Nonius AXS Inc. **2004**, Madison, Wisconsin, USA.

(63) Sheldrick, G. M. *SHELXS-97, Program for Crystal Structure Solution*; University of Göttingen, Göttingen, Germany, 1997.

(64) Sheldrick, G. M. *SHELXS-97, Program for Crystal Structure Refinement*; University of Göttingen, Göttingen, Germany, 1997.

(65) Johnson, C. K., *Report ORNL-5138*; Oak Ridge National Laboratory, 840 Oak Ridge, TN, 1976.

(66) *International Tables for X-ray Crystallography*; Kluwer Academic Press: Dodrecht, The Netherlands, 1992; Vol. C, Tables 4.2.6.8 and 6.1.1.4.

(67) Evans, D. F. *J. Chem. Soc.* **1959**, 2003–2005.

(68) Sur, S. K. *Magn. Res.* **1989**, *82*, 169–173.

(69) Harvey, D. A.; Lock, C. J. L. *Acta Crystallogr.* **1986**, *C42*, 799–801.

(70) Pavlova, S. V.; Wen, Y. S.; Chan, S. I. *Acta Crystallogr. Sect. E* **2003**, *E59*, m792–m793.

(71) Lonnon, D. G.; Colbran, S. B.; Craig, D. C. *Eur. J. Inorg. Chem.* **2006**, 1190–1197.

(72) Addison, A. W.; Rao, T. N.; Reedijk, J.; van Rijn, J.; Verschoor, G. C. *J. Chem. Soc. Dalton Trans.* **1984**, *7*, 1349–1956.

(73) Masuda, H.; Ozols, R. F.; Lai, G. M.; Fojo, A.; Rothenberg, M.; Hamilton, T. C. *Cancer Res.* **1988**, *48*, 5713–5716.

Table of contents

Complexation of copper(II) chloride with bidentate and tridentate Paullone-based ligands HL^{1-2} and HL^{3-4} modified at the lactone function resulted in four-coordinate (**1** and **2**) and five-coordinate (**3** and **4**) copper(II) complexes, which show markedly different, but remarkably high, antiproliferative activities in human cancer cell lines with IC_{50} values in the micromolar (**1**, **2**) or in the nanomolar (**3**, **4**) concentration range.	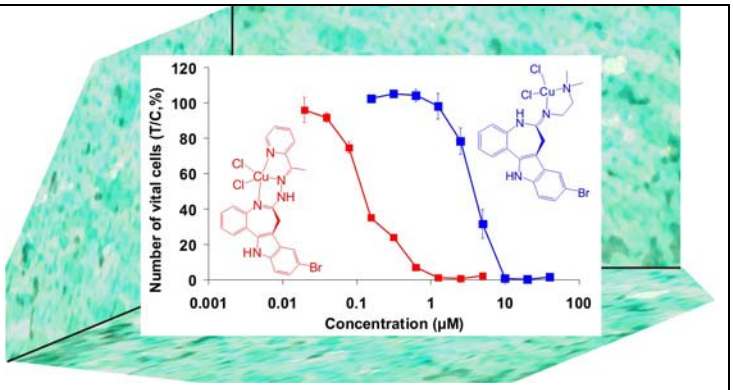

Supporting Information

Highly Cytotoxic Copper(II) Complexes with Modified Paullone Ligands

Michael F. Primik,[†] Gerhard Mühlgassner,[†] Michael A. Jakupec,[†] Olivier Zava,[‡]

Paul J. Dyson,[‡] Vladimir B. Arion,[†,*] Bernhard K. Keppler[†]

[†] Institute of Inorganic Chemistry, University of Vienna, Währinger Str. 42, A-1090 Vienna, Austria

[‡] Institut des Sciences et Ingénierie Chimiques, Ecole Polytechnique Fédérale de Lausanne (EPFL), CH-1015 Lausanne, Switzerland

*To whom correspondence should be addressed. Address: Institute of Inorganic Chemistry, University of Vienna, Währinger Str. 42, A-1090 Vienna, Austria. Phone: +431427752615. Fax: +431427752680. E-mail: vladimir.arion@univie.ac.at.

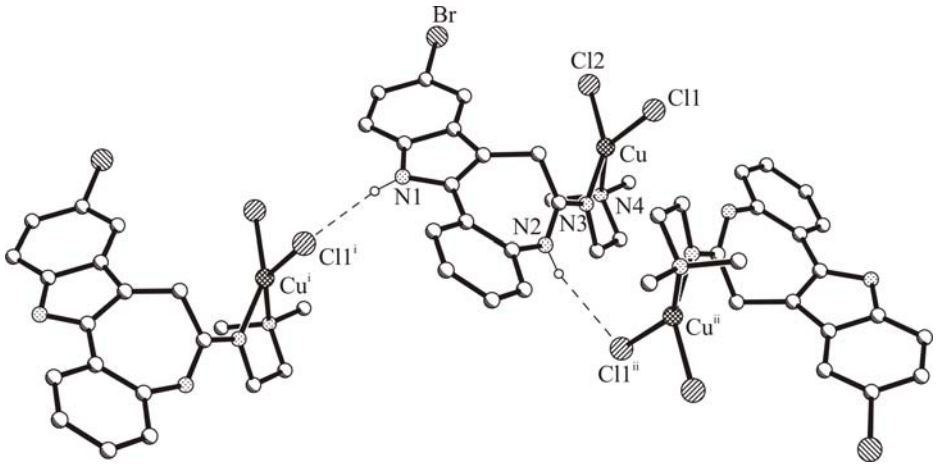

Figure S1. Part of the crystal structure of **2**, showing the intermolecular hydrogen bonding interactions. Symmetry codes: (i) *x* + 1, *y*, *z*; (ii) –*x*, –*y*, –*z*.

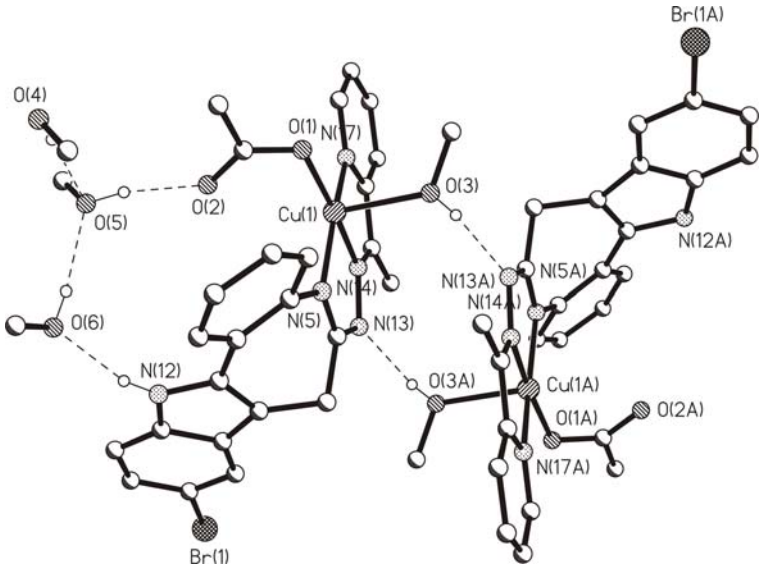

Figure S2. Part of the crystal structure of **5·3CH$_3$OH**, showing the intermolecular hydrogen bonding interactions. Symmetry codes: (i) *x* + 1, *y*, *z*; (ii) –*x*, –*y*, –*z*.

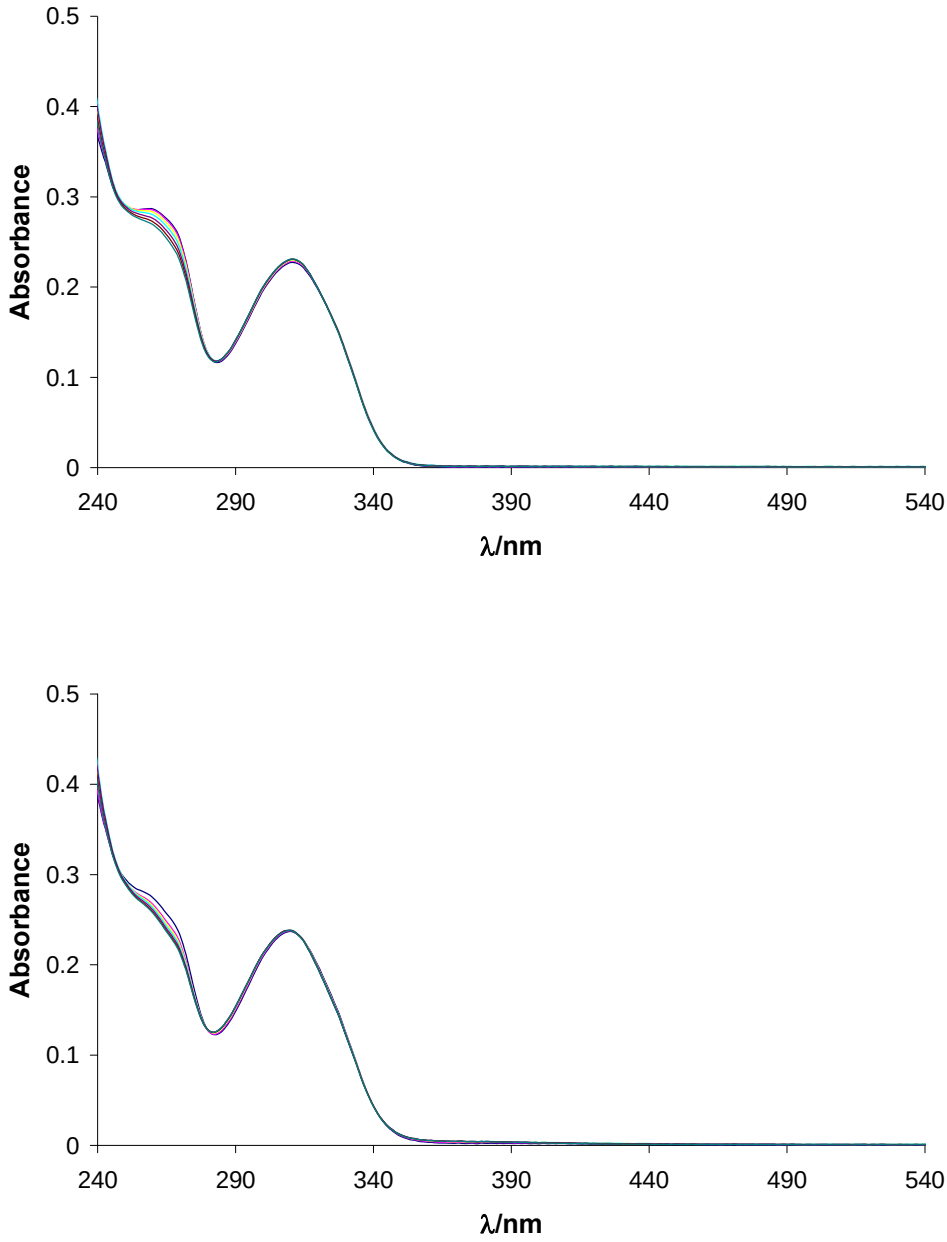

Figure S3. Time dependent UV-vis spectra of the ligand HL[1] (top) and complex **1** (bottom) in 1.25% v/v DMSO/H_2O. The spectra were measured immediately after dissolution (dark blue), after 4 h (magenta), 8 h (yellow), 12 h (turquoise), 16 h (violet), 20 h (brown) and 24 h (green).

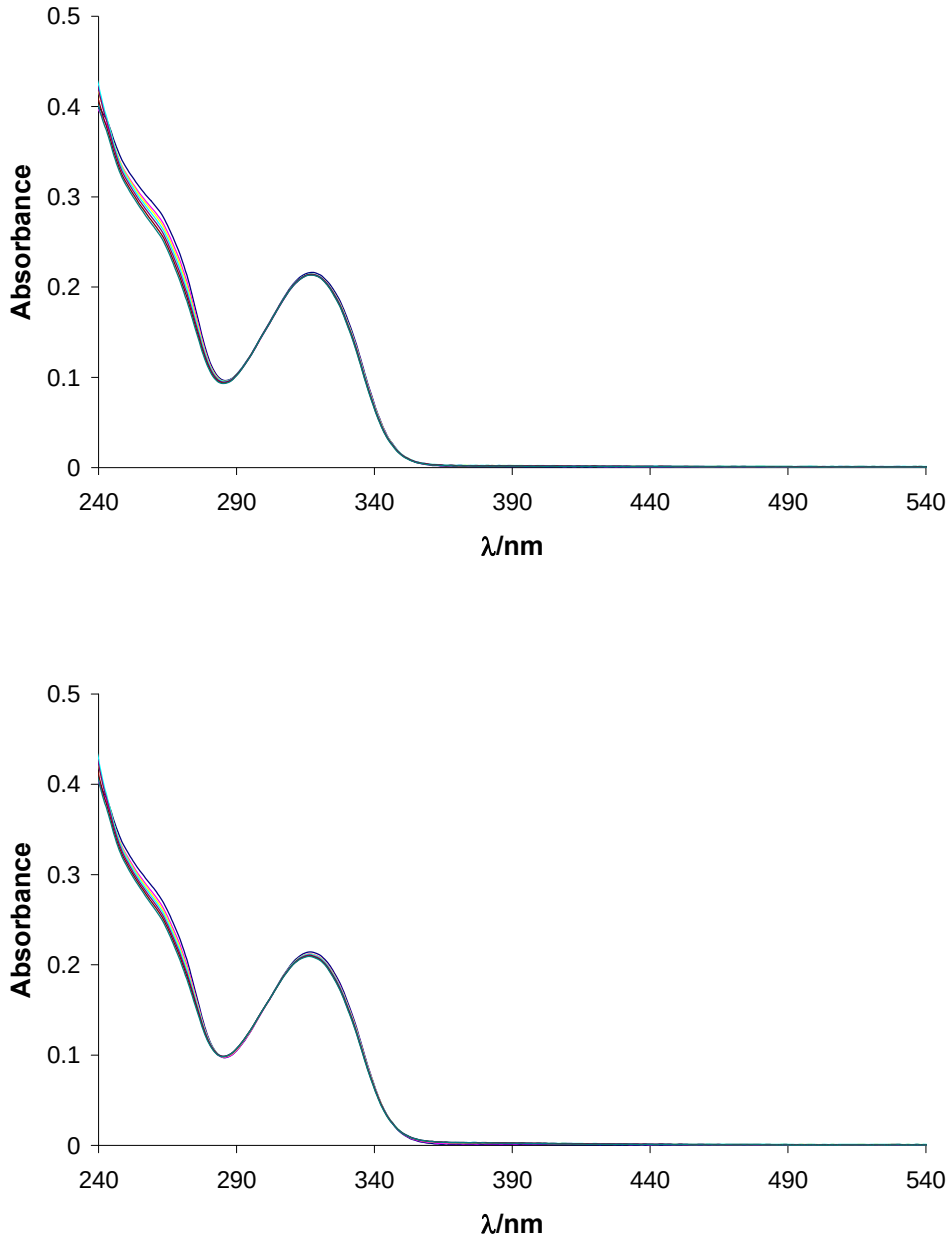

Figure S4. Time dependent UV-vis spectra of the ligand HL^2 (top) and complex **2** (bottom) in 1.25% v/v DMSO/H_2O. The spectra were measured immediately after dissolution (dark blue), after 4 h (magenta), 8 h (yellow), 12 h (turquoise), 16 h (violet), 20 h (brown) and 24 h (green).

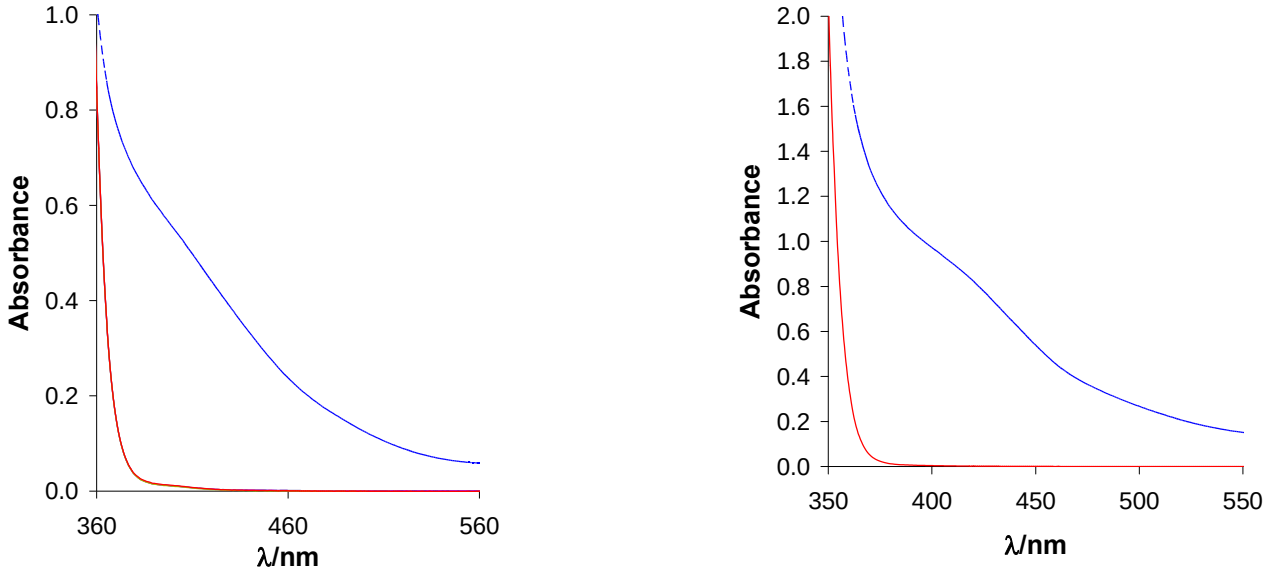

Figure S5: Charge-transfer bands of 1 mM solutions of complexes **1** (left, blue) and **2** (right, blue) in methanol compared to those of the corresponding ligands HL^1 (left, red) and HL^2 (right, red) in methanol.

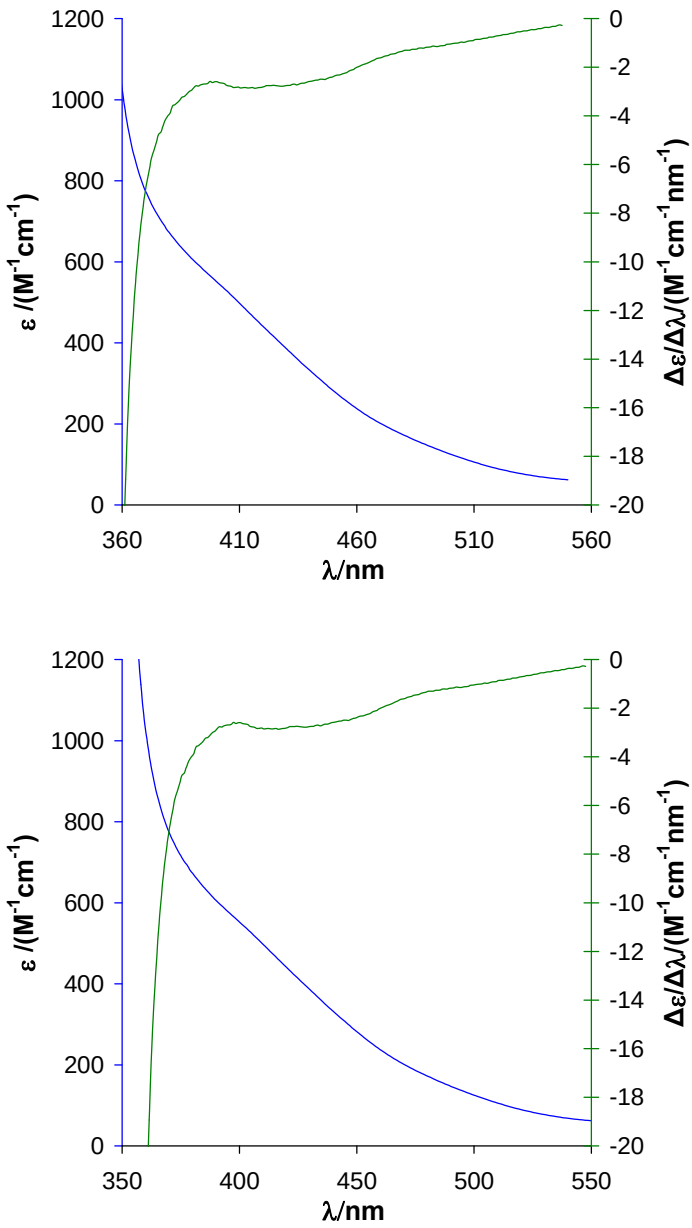

Figure S6. UV-vis spectra of **1** (top, blue) and **2** (bottom, blue). The first derivatives (green in both cases) were used to characterize shoulders (maxima of the first derivatives).

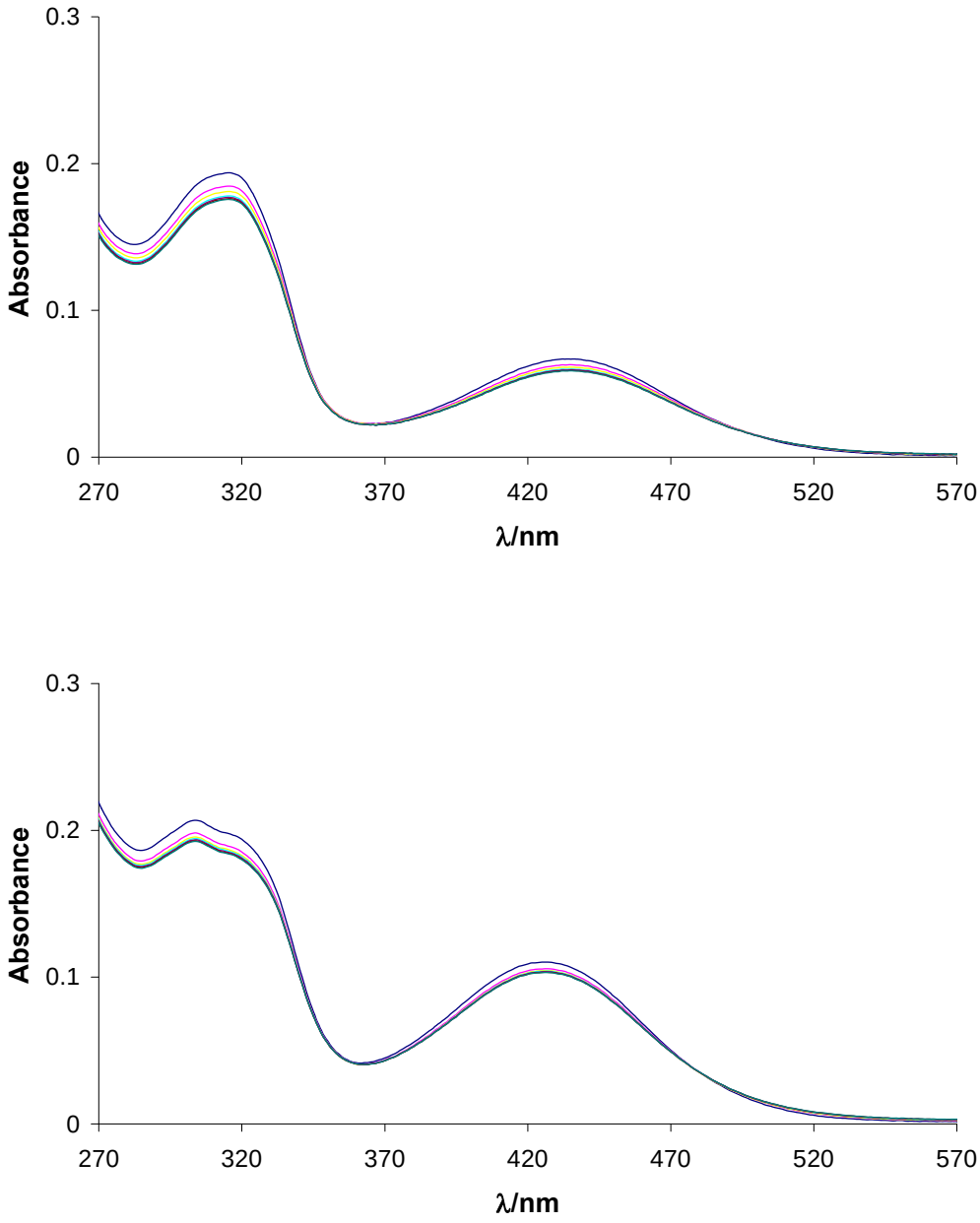

Figure S7. Time dependent UV-vis spectra of the complexes **3** (above) and **4** (below) in 10% v/v DMSO/H_2O. The spectra displayed were recorded immediately after dissolution (dark blue), after 4 h (magenta), 8 h (yellow), 12 h (turquoise), 16 h (violet), 20 h (brown) and 24 h (green).

Curriculum vitae

Full name	Michael Franz Primik
Date of birth	27th May 1986
Place of birth	Klagenfurt am Wörthersee
Adress	Hormayrgasse 59 / Top 7
	1170 Wien
Email	michael.primik@univie.ac.at

Education

03/2009 – present day	Diploma student at the Institute of Inorganic Chemistry, University of Vienna
10/2004 – present day	Undergraduate study of Chemistry at the University of Vienna
06/2004	A-levels with honours
2003 & 2004	Participation in the national competition of the Austrian Chemistry Olympiade
2000 – 2004	Participation in the Austrian Chemistry Olympiade courses at BG/BRG Mössingerstraße
1996 – 2004	Secondary school: BG/BRG Mössingerstraße, 9020 Klagenfurt am Wörthersee (with focus on natural sciences)
1992 – 1996	Elementary school: Volksschule 2 – Süd, 9170 Ferlach

Professional experience

10/2008 – present day	Tutor in undergraduate lab courses at the Institute of Inorganic Chemistry, University of Vienna
04/2009 – 05/2009	Fellowship study at the Department of Inorganic and Analytical Chemistry of the University of Szeged, Szeged, Hungary
07/2008	Research scholarship at the Institute of Inorganic Chemistry, University of Vienna

08/2007 – 09/2007	Practical at Donau Chemie AG, 9371 Brückl
08/2005 & 07/2006	Practical at Institut für med. und chem. Labordiagnostik, LKH Klagenfurt, 9020 Klagenfurt am Wörthersee
summers 2003 & 2004	Various summer jobs

Language skills	German, native language English, A-level niveau Italian, A-level niveau
Computer skills	MS Office and OpenOffice Several chemical softwares (ChemDraw, etc)
Interests	Member of the volunteered fire brigade Glainach-Tratten, 9170 Ferlach Member of the VFÖC (Verein der Freunde der Österreichischen Chemieolympiade) Football (soccer) and Icehockey, active and passive Table Top Strategy Games and accordant modeling and painting